Sequenced Crop Evapotranspiration and Water Requirement in Developing a Multitrigger Rainfall Index Insurance and Risk-Contingent Credit

MICHAEL K. NDEGWA,[a] APURBA SHEE,[a] CALUM TURVEY,[b] AND LIANGZHI YOU[c,d]

[a] *Department of Food and Markets, Natural Resources Institute, University of Greenwich, London, United Kingdom*
[b] *Department of Applied Economics and Management, Cornell University, Ithaca, New York*
[c] *Environment and Production Technology Division, International Food Policy Research Institute, Washington, D.C.*
[d] *Macro Agriculture Research Institute, College of Economics and Management, Huazhong Agricultural University, Wuhan, Hubei, China*

(Manuscript received 27 April 2021, in final form 1 September 2021)

ABSTRACT: Weather index insurance (WII) has been a promising innovation that protects smallholder farmers against drought risks and provides resilience against adverse rainfall conditions. However, the uptake of WII has been hampered by high spatial and intraseasonal basis risk. To minimize intraseasonal basis risk, the standard approaches to designing WII based on seasonal cumulative rainfall have been shown to be ineffective in some cases because they do not incorporate different water requirements across each phenological stage of crop growth. One of the challenges in incorporating crop phenology in insurance design is to determine the water requirement in crop growth stages. Borrowing from agronomy, crop science, and agrometeorology, we adopt evapotranspiration methods in determining water requirements for a crop to survive in each stage that can be used as a trigger level for a WII product. Using daily rainfall and evapotranspiration data, we illustrate the use of Monte Carlo risk modeling to price an operational WII and WII-linked credit product. The risk modeling approach that we develop includes incorporation of correlation between rainfall and evapotranspiration indices that can minimize significant intertemporal basis risk in WII.

KEYWORDS: Africa; Precipitation; Rainfall; Evapotranspiration; Insurance

1. Introduction

In sub-Saharan Africa (SSA), agriculture is largely practiced by smallholder farmers, is predominantly rain fed, and is exposed to covariate weather and related risks including frequent drought leading to significant yield losses and, at times, to total crop failure (Carter et al. 2014; Leblois and Quirion 2013; Patt et al. 2010; Shiferaw et al. 2011; Vroege et al. 2021a). Efforts have been made to mitigate crop yield risks by introducing insurance products using various forms of weather index insurance (WII). These have been favored over ''all peril'' crop insurance for a variety of reasons including adverse selection, moral hazard, and transactional costs (Benami et al. 2021; Carter et al. 2007; Glauber 2004; Hazell 1992; Skees et al. 1999; Skees and Barnett 2006; Vroege et al. 2021a). The objective of WII is to establish a trigger below (or above) which the weather peril is highly correlated with yield loss. The most common index is based on cumulative rainfall over a season (Giné and Yang 2009; Karlan et al. 2014; Shee and Turvey 2012; Shee et al. 2019) although other notable indices have been proposed including average area yield (Carter et al. 2007), soil moisture (Vroege et al. 2021b), heat index (Leppert et al. 2021), vegetation indices such as the normalized difference vegetation index (NDVI) and enhanced vegetation index (EVI; Chantarat et al. 2013), and commodities prices (Karlan et al. 2011; Shee and Turvey 2012).

Although promising and showing favorable results where adopted, index insurance has generally experienced frustratingly low uptake levels and widespread commercial upscale is yet to be realized. Two factors have been identified as the cause for the poor uptake of the products: 1) liquidity constraints, affordability, and willingness to pay among the small-scale farmers (Ali et al. 2020; Binswanger-Mkhize 2012; Casaburi and Willis 2018; Chantarat et al. 2017; Liu et al. 2020; Smith and Watts 2019); and 2) inherent intertemporal and spatial basis risk (Barnett and Mahul 2007; Jensen and Barrett 2017, 2016; Norton et al. 2012; Tadesse et al. 2015).

Agricultural and development economists are shifting focus to index insurance bundled with agricultural loans to address farmers' liquidity constraints and affordability issues. Although promising, the challenges of basis risk remain, which affects confidence among farmers, insurers, banks, and other stakeholders in the sector. To minimize intraseasonal basis risk, the standard approaches to designing WII based on seasonal cumulative rainfall have shown to be ineffective as they do not incorporate water requirements in each stage of a crop growth (Bucheli et al. 2020; Shi and Jiang 2016; Turvey 2001; Turvey et al. 2019). To design effective WII, it is important to consider crop phenology and water needed for a crop to survive in each growth stage (Conradt et al. 2015; Dalhaus and Finger 2016; Dalhaus et al. 2018).

To address problems of WII (and WII bundled credit) based on cumulative rainfall, we offer in this paper an alternative approach. Borrowing from agronomy, crop science, and agrometeorology we adapt evapotranspiration methods in determining water requirements for a crop to survive in each stage (Allen et al. 1998; Pereira and Alves 2013; Wu 1997) to the WII problem. Specifically, we evaluate WII using evapotranspiration as the triggering event rather than direct rainfall.

Corresponding author: Michael K. Ndegwa, m.k.ndegwa@greenwich.ac.uk

DOI: 10.1175/WCAS-D-21-0071.1

A number of evapotranspiration indices have been identified as good drought indicators and potentially superior weather variables that can improve upon the design of WII products (Bucheli et al. 2020; Enenkel et al. 2018, 2019; Leblois and Quirion 2013; von Negenborn et al. 2017). Evaporation has the advantage of weighting soil moisture evaporation in the early phases of plant development with little canopy cover and transpiration due to leaf surface expansion and increased ground cover in later stages. It also has the advantage of capturing the temperature variations and spikes across time and space, which has been shown to affect yields significantly (Beguería et al. 2014; Bucheli et al. 2020; Tack Barkley et al. 2017; Tack et al. 2015; Tack Lingenfelser et al. 2017; Vicente-Serrano et al. 2010).

In this paper, we first present a rainfall index insurance with specific crop evapotranspiration or water needs as the trigger variable. Similar products had been alluded to in Leblois and Quirion's (2013) review, but the specifics of how a WII contract designed around specific crop evapotranspiration is absent in literature. Unlike Bucheli et al. (2020) two evapotranspiration based indices, our approach does not require historical yield data and can, therefore, be adapted to sub-Saharan Africa and other low-income agricultural economies where a high density of small farms is normally coupled with unavailability of reliable historical farm-level and area yield data. Second, we compare the realized rainfall with a specific crop evapotranspiration across four distinct crop growth stages. In doing so, we can determine rain shortfalls at each growth stage and compute the corresponding indemnity for that growth stage. The sum of growth-stage indemnities provides the entire seasonal indemnity. We then bundle the WII to a commercial agricultural loan and hence present an improved risk-contingent credit design. Last, using Program Evaluation Research Task (PERT) Monte Carlo distributions, we present a risk modeling approach to designing a WII and risk-contingent credit (RCC), which are operational in the Eastern Province of Kenya. The proposed model uses maize grown in Machakos County, Kenya, as the underlying crop, but it could be easily adapted for other crops grown in any other part of the world provided the right evapotranspiration computation methods are applied.

2. Literature and study background

a. *Developments in weather index insurance and RCC designs*

Although linking insurance to credit has been an active debate for over a decade (Binswanger-Mkhize 2012; Carter et al. 2011; Marr et al. 2016; Meyer et al. 2017; Miranda and Gonzalez-Vega 2011; Shee and Turvey 2012; Skees and Barnett 2006; Skees et al. 2007), there has only been a small number of operational insurance-linked credit products both in literature and in the field. Studies specific to bundled, or risk-contingent credit designs include Giné et al. (2008), Giné and Yang (2009), Shee and Turvey (2012), Shee et al. (2019), and Turvey et al. (2019). Giné et al. (2008) and Giné and Yang (2009) discuss and evaluate (in India and Malawi, correspondingly) an insurance bundled credit product for farm inputs whose payout is contingent to rainfall shortfall below crop water needs. They divide the season into three growth phases, namely, planting, budding/flowering, and harvesting. Shee and Turvey (2012) defined RCC as a general term for any credit instrument that imbeds within its structure a contingent claim, which when triggered transfers part or all of the borrower's liability to the lender or integrator/counterparty. They propose and evaluate an insurance-linked credit product based on pulse crops in India where loan repayment reduced as pulse-crop prices fall. Turvey et al. (2012) use a similar approach to evaluate price-linked risk-contingent credit for dairy farmers in upstate New York based on futures prices. Karlan et al. (2011) proposed and evaluated a similar (commodity price contingent) product in Ghana with maize and garden eggs and set the triggers at 7th percentile of historical year-long prices for maize and 10th percentile of historical prices during the harvest period for garden egg. Shee et al. (2019) document a drought RCC product operational in Machakos County in Kenya with an indemnity contingent on the performance of a cumulative rainfall index with a trigger based on the 15th percentile of historical rainfall measures. The product was empirically evaluated by Ndegwa et al. (2020) in the first phase of an RCT implemented in 2017/18. As documented in Turvey et al. (2019) the cumulative rainfall measure revealed unworkable weakness due to intraseasonal basis risk. This required a redesign based on a multiple-event dynamic trigger model, that was used in the second implementation of RCC in 2019/20. Mishra et al. (2020) evaluate the effect of rainfall index insurance on loan application by farmer groups and loan offering by rural and community banks (RCBs) in Ghana. They bundled conventional agricultural loans from RCB with existing index insurance contracts for maize from the Ghana Agricultural Insurance Programme—a multitrigger WII dividing the season into three phases, which plays out based on the number of consecutive dry days during germination, germination to flowering onset, and flowering periods.

A more recent literature has examined the distribution of rainfall and other weather variables in the form of multiple events WII across phenological growth stages (Turvey et al. 2019). In their composite WII design, Shi and Jiang (2016) divided rice growth into six distinctive stages and assumed that the duration of the growth stages remains unchanged over the 20-yr time series they used to design their product. Working with wheat from Germany, Dalhaus and Finger (2016) found that use of crop phenological growth stages reduced temporal basis risk and hence significantly increased expected utility. Acknowledging that the start and end of a season and that of growth stages are not static over the years, Conradt et al. (2015) proposed a flexible WII design using growing degree-days (GDD) to determine annual variable start and end dates for the insured period. They rated the design with wheat from Kazakhstan and concluded that introduction of flexibility reduced basis risk significantly. Dalhaus et al. (2018) conducted a comparative analysis between using publicly available phenology reports and GDD to determine the start and end of wheat (in Germany) growth stages and found that use of phenological reports significantly reduced basis risk while GDD did not. The somewhat contradicting findings between Conradt et al. (2015) and Dalhaus et al. (2018) on use of GDD

is a clear indication that weather variations across the globe necessitate contextual assessment and documentation of varied approaches of addressing basis risk and hence objectively chose the locally fitting methods. To address the erratic and consistent nature of rainfall within a season, Turvey et al. (2019) proposes a product based on 21-day overlapping cumulative rainfall. They define specific events as 21 fixed days that are overlapping in measurement but nonoverlapping in indemnity, which implies a multievent dynamic trigger that can only indemnify once within a period of 21 days. Although the start and end of seasons are static in their model, the 21 days periods are not and starts to count once an indemnity has been triggered. However, as noted by Odening et al. (2007) and Odening and Shen (2014), efforts to minimize basis risk often increases the complexity of the WII products, which can lead to low insurance uptake. The trade-off between reducing basis risk and avoiding complexity requires the use of the transparent and easy to understand designs, which at the same time mitigates farmers exposure to basis risk (Dalhaus and Finger 2016; Leblois 2014; Patt et al. 2009).

In this study, we present improved WII and RCC designs where we propose the use of crop evapotranspiration to innovatively design a trigger mechanism for rainfall index insurance. To minimize intratemporal basis risk, we cumulate our design variables within Allen et al's. (1998) four distinct growth stages, namely, initial, development, mid, and late stages. These stages have been used for a long time to determine and schedule irrigation needs but we for the first time apply the approaches to WII design.

b. *The study area*

For empirical application and rating of the proposed WII and RCC designs, we work with historical rainfall and evapotranspiration data from 11 distinct divisions of Machakos County, Kenya. The county is located in the eastern region of Kenya, and it covers roughly 6000 km^2. It is a diverse county categorized into five agroecological zones, but largely arid and semiarid, with annual rainfall ranging between 500 and 1300 mm (averaging around 700 mm) and temperature ranging between 18° and 29°C (Jaetzold et al. 2010; Ministry of Agriculture, Livestock and Fisheries 2017). Rainfall in this county is bimodal with the short rains normally coming between March and May (first season) and the long rains between October and December (second season). Agriculture is the mainstay of livelihoods in Machakos County, employing about 73% of the population and contributing approximately 70% to the household incomes (Ministry of Agriculture, Livestock and Fisheries 2017). Approximately 60% of the land is arable, largely cultivated with food crops such as roots, cereals (primarily maize), and legumes (mostly beans and cow peas). Production is mostly small-scale subsistence, predominantly rain fed and subject to recurrent drought.

In Machakos, farmers grow either early maturing (100–125 days) or extra early maturing (90–110 days) maize varieties. Extra early maturing varieties continue to gain prominence in the county due to increasing aridity and poor rainfall distribution where late arrival and early ending of the rains is a common phenomenon. For the proposed insurance product, we shall work with the historical long rain season, which occurs from mid-October to mid-January and consider the extra early maturing varieties taking 90 days to reach physiological maturity. The model can, however, be adapted to short rain seasons as well as varieties that take longer to reach physiological maturity.

3. Evapotranspiration approaches in determining water requirement for crop growth stages

a. *Evapotranspiration concept: A case of maize crop*

It has been established that for optimal yield, maize requires 500–800 mm of water during its total growing period of 90–110 days for extra early maturing, 125 days for early maturing and 180 days for late maturing varieties (Critchley et al. 1991). These are approximate as moisture use varies from farm to farm, season to season, growth stage to growth stage as well as day to day. For maize, consumptive use increases with plant growth where it peaks at flowering and watery grain filling stages and starts to decline when grain moisture loss starts as the crop approaches physiological maturity.

Moisture deficit (receiving less than required) at any growth stage has negative effects on yields but stages such as germination, flowering, and grain filling are more critical than others. The crop water requirement is the amount of water required by a plant to replenish what has been lost to the atmosphere through two concomitant but independent natural processes, namely, evaporation and transpiration, which combined, result in evapotranspiration. Evaporation is the loss of moisture from soil surface to the atmosphere while transpiration is the loss of moisture directly from the crop via the stomata to the atmosphere. Evaporation is more important from planting through seedling stage while transpiration becomes more important as plants gain leaves and cover the ground more and more. Increase in transpiration due to leaf surface expansion results in reduced direct evaporation from the soil surface.

Evapotranspiration methods have been widely used for decades among agronomists, water and agricultural (biosystems) engineers and agrometeorologists to determine crop water requirements and manage water resources including irrigation (Wu 1997). Here, irrigation can be defined by the fraction of crop water requirement not satisfied by rainfall, soil water storage and groundwater contribution (Pereira and Alves 2013). In this case, irrigation can be thought of as an insurance investment against drought but in reality, maize fields in Kenya and other low-income countries are rarely irrigated, especially among the smallholder farmers.

In the context of this paper, the same crop water requirement and evapotranspiration approaches will be used in designing the insurance trigger for rainfall index insurance. Our design has the potential to eliminate basis risk resulting from erratic rainfall patterns and rainfall-based triggers. The advantage of this approach is that water deficit will be an indicator of the drought intensity and hence the payout amount. The water requirement measures can be sequenced along the

key distinctive crop growth stages to design a multitrigger or multiple event index insurance.

b. *Evapotranspiration computation methods*

To estimate crop water requirement using evapotranspiration, the following equation is used for all type of crops in different geographic and agroecological zones (Allen et al. 1998):

$$\text{ETcrop} = K_c \times \text{ETo}, \tag{1}$$

where ETcrop (or ETc) is specific crop evapotranspiration (mm t^{-1}), ETo is the reference crop evapotranspiration (mm t^{-1}), t represents time scale, and K_c is a specified crop factor that is used as the conversion coefficient to compute/recover a crop (maize in this case) specific evapotranspiration from the ETo for a given area and time period. The specific crop coefficients for different growth stages are experimentally obtained in field trials using

$$K_c = \frac{\text{ETcrop}}{\text{ETo}}. \tag{2}$$

Examples of such experimental field trials include Djaman et al. (2018), Piccinni et al. (2007), and Piccinni (2009). Lysimeters are used to measure crop water use (ETcrop) throughout the growing season. ETo for the same period is measured directly from a reference crop such as a perennial grass or computed from weather data using methods such as Penman–Monteith, Hargreaves, and Blaney–Criddle. In this study, we use the FAO predetermined crop-specific K_c coefficients available in Table 17 of Allen et al. (1998) for different crops at different key growth stages.

The reference evapotranspiration (ETo) is the evapotranspiration of a disease-free crop grown from a reference surface that is not short of moisture and fertility (Allen et al. 1998; Pereira and Alves 2013). Remote sensing reference evapotranspiration data is freely available from different weather and Earth surveillance sites, and, when compared with K_c-based evapotranspiration estimations, remote sensing methods have a strong advantage in spatial accuracy because of the estimation of evapotranspiration for each pixel of a satellite image, using observed reflected radiation and temperature (Lorite et al. 2018). However, the readily available evapotranspiration data only dates to 2000. In a situation like ours, where longer historic data is preferred, reference evapotranspiration can be computed using some existing methods if the required climate variables, particularly temperature and extraterrestrial radiation, are available. Once ETo has been either obtained or computed, it is then entered into the ETcrop equation above to compute crop evapotranspiration or the crop water requirement.

There are several empirical approaches to calculate reference evapotranspiration for a given area that have been tested and compared for their applicability in different climatic conditions around the globe and appropriate recommendations made. Of the many, the FAO Penman–Monteith equation (Allen et al. 1998) is the most recommended but has two shortcomings; namely, it is a complex method requiring more climate variables and it ideally should be used with in situ weather stations data. The paucity of such data in SSA countries and other low-income countries where weather stations are few and far between hampers the application of this method. However, using the meteorological data from nearby stations, this method is mostly used to calibrate the results from the other simpler and more pragmatic methods for such regions where physical weather stations data are not available.

There are many alternative methods estimated with both physical stations and remote sensing meteorological data. They come with different features that make them ideal for different climatic conditions with some of them being limited in terms of widespread application. Two approaches among them stand out for consideration in this study. They are Hargreaves method developed by Hargreaves and Zohrab (1985) and Blaney–Criddle method developed by Blaney and Criddle (1962). Both have been widely recommended where only air temperature data are available and for arid and semiarid areas (ASALs). They also are straightforward and convenient approaches to work with. Of the two, Hargreaves method is considered to be a superior approach in tropical ASALs, and we chose it for our study (Allen et al. 1998; Maeda et al. 2011; Tabari 2009; Zhao et al. 2010). Hargreaves ETo is given by

$$\text{ETo} = 0.0023\text{RA}(T_{\text{max}} - T_{\text{min}})^{0.5}(T_{\text{mean}} + 17.8), \tag{3}$$

where ETo is the reference evapotranspiration (mm day^{-1}), RA is the extraterrestrial radiation, T_{mean} is mean temperature, T_{max} and T_{min} are respectively the maximum and minimum air temperature that is the average of all the daily maximum or minimum (respectively) temperatures recorded for the respective time period.

c. *Sequencing the* ETc *and rainfall at key maize growth stages*

In the crop water requirement literature, growth of all crops from planting to full maturity has been divided into four main stages, namely, initial, development, midseason, and late-season stages (Allen et al. 1998). Further, the number of days each crop takes per stage have been empirically estimated as well as the key milestones the crop achieves within each stage. Transferable crop factor (K_c) values for computation of ETcrop from ETo have also been empirically estimated for specific crops at different growth stages where it is recommended that crop water requirement be calculated stagewise or for shorter periods, especially for the determination of the deficit that can be met by irrigation means. Table 1 shows the growth stages for early and extra early maturing maize varieties grown in the semiarid areas, the number of days, and the K_c values for each stage.

We use this information to calculate the stagewise[1] water requirement for maize in all the sub counties of Machakos

[1] Weekly averaging with Hargreaves method has also been found to yield consistent results (Hargreaves and Allen 2003; Wu 1997) and can yield a superior trigger and cover for the farmers as opposed to longer time aggregations such as months or growth periods. This will, however, be a computationally cumbersome model and where cumulation is used as opposed to moving averages, the difference may be inconsequential.

TABLE 1. Maize growth stages, number of days, and the associated K_c values. Allen et al. (1998) provides K_c values and growth-stage periods based on varieties taking 125 days to reach physiological maturity. We use this base information to compute the number of days for other varieties by converting the stagewise number of days for 125-day varieties as proportions and apportioning them to the rest accordingly. The K_c values do not change. We augment this information with our focus group discussions with the community where we collected the days for various growth stages for maize, capturing different varieties currently grown.

Growth stage	Initial	Development	Midseason	Late season
K_c	0.4	0.8	1.15	0.7
125 days to maturity	20	35	40	30
120 days to maturity	19	34	38	29
110 days to maturity	18	31	35	26
100 days to maturity	16	28	32	24
90 days to maturity	14	25	29	22

County from 1983 to 2019 and then compare this with the actual rainfall for the same period and geographic area to determine whether the maize received enough rainfall and, if not, determine the deficit in millimeters per meter squared. We therefore design a multitrigger WII where indemnity determination is made at growth-stage level. The proposed design is also in line with latest developments in WII designs where sequencing the weather variables and the index as opposed to seasonal cumulative is advised (Turvey et al. 2019).

Figure 1 shows the time series of rainfall and maize evapotranspiration using Yathui Division as an example. Rainfall volatility is considerably higher than maize evapotranspiration or water requirement, which seems to be steady over the years and for all the growth stages. Figure 2 compares growth-stage cumulation with seasonal cumulation of rainfall and maize evapotranspiration for four years (2015–18) using Yatta Division as an example. Growth-stage cumulations capture the temporal variations that are lost when cumulation is done at season level. With seasonal cumulation, rainfall received was sufficient to meet the seasonal-level maize water requirement for the four years considered. However, rainfall distribution in Machakos and other ASALs is erratic with crops frequently experiencing moisture stress in some growth stages. This can lead to diminished yields that often cannot be detected by seasonal rainfall cumulations. Yield shortfalls uncorrelated with the weather index is referred to as basis risk.

d. *Weather data sources and processing*

Following the Hargreaves method to calculate reference evapotranspiration, we needed maximum, minimum, and mean air temperature, along with extraterrestrial radiation. Maximum, minimum, and mean air temperature data were extracted from ERA5 hourly data on single levels from 1979 to the present (https://cds.climate.copernicus.eu/cdsapp#!/dataset/reanalysis-era5-single-levels?tab=overview); ERA5 is a state-of-the-art climate dataset with a resolution of 0.25°, produced by the European Centre for Medium-Range Weather Forecasts (ECMWF 2019). As a reanalysis dataset, it couples model data with observation data to create temporally and spatially

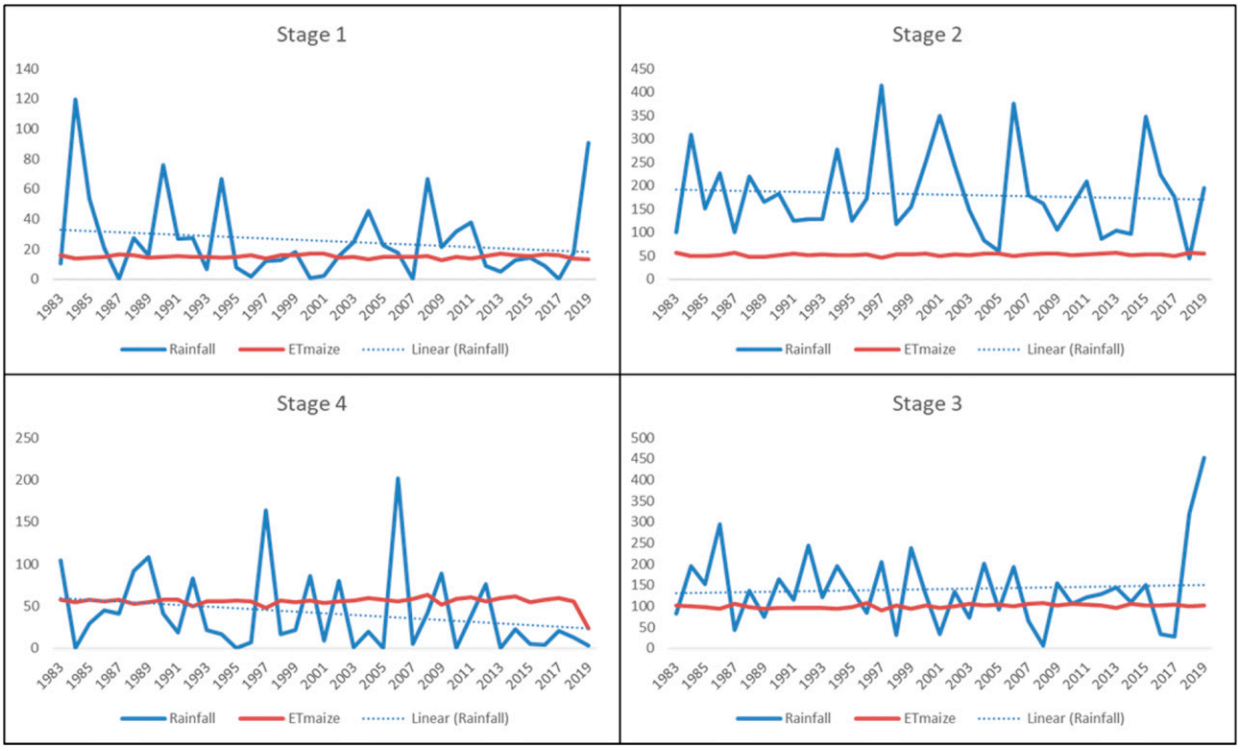

FIG. 1. Yathui Division growth-stage rainfall and ETmaize time series from 1983 to 2019.

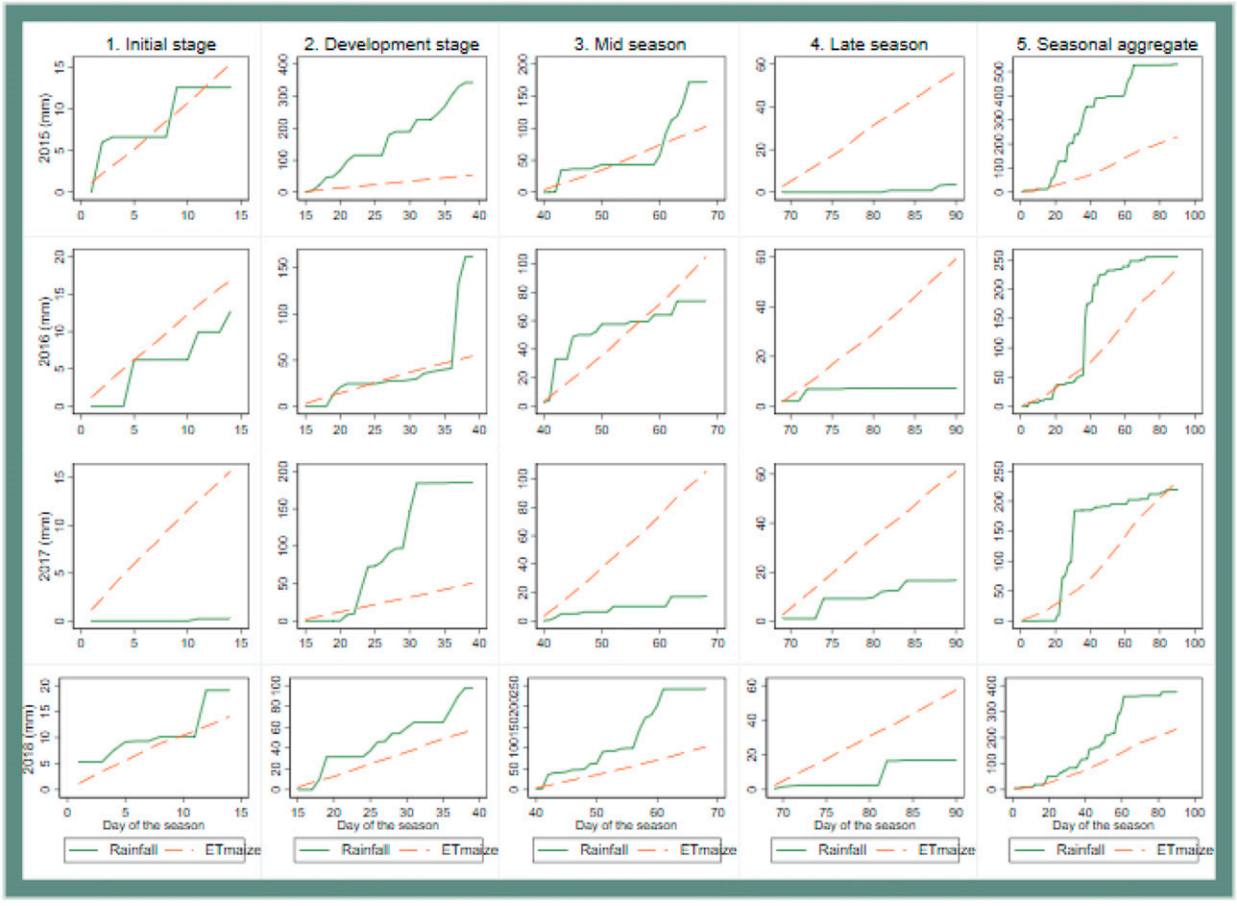

FIG. 2. Growth stages and seasonal cumulation of rainfall and ETmaize for 2015–18 for Yatta Division.

consistent simulations spanning back decades. We access the ERA5 dataset through Google Earth Engine.[2] A shapefile of divisions administrative boundaries was overlaid on ERA5 variables to capture maximum, minimum, and mean air temperature 2 m above the Earth surface. Google Earth Engine first rasterizes the administrative boundaries to the same scale of ERA5 data (0.25°, i.e., ~30 km), and then aggregates the pixels of ERA5 data by computing the mean if their centroids are covered by the boundaries. Temperature data from these sources come in kelvins. For our calculations, we convert them to degrees Celsius by subtracting 273.15: $[T(°C) = T(K) - 273.15]$.

Following the equations and process documented in Allen et al. (1998), extraterrestrial radiation (RA) for each day of the year were calculated using the solar constant, the inverse relative Earth–sun distance, the sunset hour angle, the solar declination, latitude, and the number of the day in the year. For latitudes, we use latitudes of the centroids of divisions boundaries as an approximation. The process of calculating RA in millimeters per day is shown in Appendix A.

For rainfall, we use Climate Hazards Center Infrared Precipitation with Station Data (CHIRPS; https://data.chc.ucsb.edu/products/CHIRPS-2.0/) 0.05° gridded precipitation data covering the majority of the world (50°S–50°N) from 1981 to near present (Funk et al. 2015). It is created by calibrating satellite imagery utilizing in situ station data, which improves accuracy. We use the version-2.0 global daily set. The CHIRPS data were processed in Google Earth Engine. The administrative boundaries at divisions level of Machakos County were overlaid on CHIRPS precipitation data. Google Earth Engine first rasterize the administrative boundaries to the same scale of CHIRPS data (0.05°, i.e., ~5.5 km), and then aggregates the pixels of precipitation data if their centroid is covered by the boundaries. The CHIRPS dataset has one image in "GeoTIFF" format for each day; for each day, we computed the mean value of all the pixels located within division and use that as the average precipitation at the respective division. The function was mapped over all the desirable dates to create time series daily rainfall data from 1983 to 2019, which were then exported in delimited format. In summary, average precipitation was extracted for each division at each day between 1 January 1983 and 31 December 2019.

[2] Google Earth Engine is an online platform that not only hosts an abundant repository of satellite imagery and geospatial datasets but also provides extraordinary computation power for data processing, supported by Google's cloud infrastructure.

4. Multitrigger WII and RCC designs

a. Defining the index, strike, and indemnifiable losses

We have growth stages t (1–4) within each season T per year j. To achieve a sequenced measure of our index and trigger variables, we work with growth stage t, cumulative rainfall index I, and maize crop evapotranspiration (ETc) within a specified season T. This will mitigate intertemporal basis risk significantly relative to season-level cumulation as has been the norm.

In general terms, a farmer who buys index insurance receives a payout from the insurer if the index I is less than a predetermined strike/trigger level S. In most index insurance design, the strike level has been set as a percentage of the historical average of the underlying index variable representing a point below which a farmer would experience significant losses warranting a payout.[3] We depart from this approach and use rainfall as our primary index variable and maize crop evapotranspiration (ETc) as a trigger variable.

In WII design, yield Y_{igT} can be looked at as a function of the index, other weather variables ω_{gtT}, which may not be captured by the index, and a host of farm/household idiosyncratic traits x_{igtT} and unobservable household and farm heterogeneity ε_{igtT}:

$$Y_{igT} = f(I_{gtT}, \omega_{gtT}, x_{igtT}, \varepsilon_{igtT}). \tag{4}$$

In our case, I_{gtT} is a rainfall index that represents the actual rainfall realized in area/division g during the growth stage t in season T. However, maize crop from division g requires ETc_{gtT} amount of water during growth stage t for optimum yield, but in some instances, rainfall falls below the required amount. A sequenced drought index insurance should be able to measure the losses incurred in a rain-fed agricultural system when rainfall falls below the required amount during a specific growth stage or when ($I_{gtT} < \text{Etc}_{gtT}$). Therefore, growth-stage rainfall shortage D associated with the choice index I can be expressed as the difference between the trigger variable ETc and the realized rainfall index I:

$$D_{gtT} = \text{ETc}_{gtT} - I_{gtT}. \tag{5}$$

The rainfall shortfall expression above would detect all levels of rainfall shortfall and hence trigger a payout even when rainfall deficiency is not large enough to cause adequate damage to warrant indemnity.[4] It would be an appealing product to the farmers in terms of level of coverage but the high indemnity probability results in exorbitantly high premiums that farmers may not afford or even be willing to pay (see Shee et al. 2020 for the trade-off between coverage and price). To capture economic losses only high enough to warrant an insurance indemnity and hence lead to reasonable payout probabilities and premiums, we design a trigger/strike level S based on ETc_{gtT} and discount it by a factor τ where $0 < \tau \leq 1$. We therefore propose a rainfall index insurance based on the rainfall probability distribution below an evapotranspiration-based trigger S, which is given by

$$S_{gtT} = \text{ETc}_{gtT} \times \tau, \tag{6}$$

and hence we can express the indemnifiable losses as adjusted rainfall shortage by

$$D^{e}_{gtT} = (\text{ETc}_{gtT} \times \tau) - I_{gtT} = S_{gtT} - I_{gtT}. \tag{7}$$

For a trigger S_{gtT}, we set our τ at 0.3 to best capture cumulative growth-stage rainfall deficiency below 30% of maize water requirement ETc_{gtT}. A quick check shows 0.49 (49%) payout probability, which resonates with the study area where diminished yields due to recurrent droughts is commonplace, a true reflection of ASALs in Africa. The probability would come down significantly when the insurance product is based on data from areas receiving higher and well distributed rainfall, and the reverse is true.

In agricultural insurance and finance, one may be interested in hedging either 1) the capital, and assuming this was borrowed, then RCC is implied, or 2) yield losses where sum insured is based on the estimation of the value of the anticipated yields in the absence of drought. The choice of what to cover against drought, either the credit/investment or yields, determine the tick value, which is the monetary value of each unit loss, in this case, each millimeter below the trigger S_{gtT}. We define the tick as the ratio of sum insured to the trigger variable (ETc). Below, we present a design purely for RCC. This can be scaled to a farm yield stand-alone insurance product by use of appropriate tick value.

b. RCC—A design purely for agricultural loans

We define tick value for agricultural credit as

$$\delta_{gtT} = \frac{f}{\text{ETc}_{gtT}}, \tag{8}$$

where f is the loan principal, the actual amount advanced to the farmer by a bank for agricultural production at the beginning of a season, and hence the sum insured. A farmer who took credit f at the beginning of a season qualifies for an indemnity λ_{gtT} at the end of each growth stage whenever the cumulative rainfall during growth period t in season T falls below the trigger S_{gtT}. Following Bucheli et al. (2020), Martin et al. (2001), Ozaki (2009), and Turvey (2001), the payout determination of a WII follows the European put option design and hence the growth-stage indemnity λ_{gtT} is given by

[3] For instance, Shee and Turvey (2012) and Shee et al. (2019), in studies contemporary to this one, proposed RCC and used rainfall as the index and set the trigger at 15th percentile of the cumulative rainfall realized at the end of the season. In their improved RCC model, they developed a dynamic trigger based on 21-day moving average of historic rainfall records and set the trigger at 60% (Turvey et al. 2019). Bucheli et al. (2020) compared different indices with lower partial moments set at the level of the respective index that coincide with 30% of yield for a specific farm.

[4] A quick check with historical rainfall and ETc data from 11 subcounties of Machakos County in Kenya produced 0.91 (91%) indemnity probability, resulting in 32.7 of 36 years covered in the study (1983–2019).

$$\lambda_{gtT} = \delta_{gtT} \times \max[(S_{gtT} - I_{gtT}), 0]. \quad (9)$$

At the end of the season, a farmer with the multitrigger RCC will be indemnified according to the sum of all the growth-stage indemnities within a specified season T in division/area/region g:

$$¥_{gT} = \sum_{i=t=1}^{n=4} \{\delta_{gtT} \times \max[(S_{gtT} - I_{gtT}), 0]\} = \sum_{i=t=1}^{n=4} \lambda_{gtT}, \quad (10)$$

where the insurer deposits the payout in the farmer's loan account directly at the end of the loan contract or once the indemnity determination has been made.

To compute actuarially fair premiums, we compute the arithmetic mean of season-level payouts over the years ($j = 1, j = 2, \ldots, j = n - 1$):

$$\rho_{gTj} = \frac{¥_{gT,j=1} + ¥_{gT,j=2} + ¥_{gT,j=3} + \cdots + ¥_{gT(j=n-1)}}{n-1}, \quad (11)$$

which can be simplified as

$$\rho_{gTj} = \frac{1}{n-1} \times \sum_{j=1}^{n-1} ¥_{gTj}. \quad (12)$$

Ideally, with microinsurance, a policy holder is required to pay up the premium amount ρ to the insurer at the beginning of the contract, or in this case at the point of taking the loan. Because many small-scale farmers are liquidity constrained (Ali et al. 2020; Chantarat et al. 2017; Liu et al. 2020; Smith and Watts 2019) we add the insurance premium to the loan principal ($f + \rho$). The bank then remits the premium amount to the insurer at the beginning of the season when the loan is taken and charges standard interest x^* on the new composite figure. We therefore define the present value of loan repayment for farmer i from division/area g in season T in year j as

$$°F_{igTj} = (f_{igTj} + \rho_{gTj})e^{x^*T} - ¥_{gTj}. \quad (13)$$

c. Risk modeling with PERT Monte Carlo distribution

To achieve greater precision and robustness in the computation of actuarially fair premiums, we present a risk modeling approach to designing a WII and RCC and propose the use of probability distributions from where one can draw infinite occurrences of different possible rainfall and evapotranspiration outcomes in line with the asymptotic theory. Since both rainfall and evapotranspiration vary over time and space, we treat both as random variables. Nevertheless, we have observed an almost perfect and positive spatial correlation for both variables and negative bivariate correlation between them (see the correlation matrices in Tables B1, B2, and B3 in appendix B). As such, we apply both spatial and bivariate correlated probability distributions where we correlate all the divisions in Machakos and also correlate rainfall and evapotranspiration within each division. Using the "@RISK" distribution fitting features, we model spatially and bivariate correlated PERT Monte Carlo distributions for both rainfall and evapotranspiration separately, discount the evapotranspiration by our τ term as illustrated in Eq. (6) and hence compute a random indemnifiable rainfall shortfall in Eq. (7) $\{\max[(\mathrm{ETc}_{gtT} \times \tau) - I_{gtT}, 0]\}$. Combining the rainfall and evapotranspiration distributions gives us a new distribution for the indemnifiable rainfall shortfall with the following four properties:

$$\text{mean: } \overline{D^e_{gtT}} = E(S_{gtT} - I_{gtT}) = E(S_{gtT}) - E(I_{gtT}) = \mu_{S_{gtT}} - \mu_{I_{gtT}}, \quad (14)$$

$$\text{variance: } \mathrm{Var}(D^e_{gtT}) = E\left[\left(S_{gtT} - \mu_{S_{gtT}}\right)^2\right] + E\left[\left(I_{gtT} - \mu_{I_{gtT}}\right)^2\right], \quad (15)$$

$$\text{covariance: } \mathrm{Cov}(S_{gtT}, I_{gtT}) = E\left[\left(S_{gtT} - \mu_{S_{gtT}}\right) \times \left(I_{gtT} - \mu_{I_{gtT}}\right)\right], \quad \text{and} \quad (16)$$

$$\text{standard deviation: } \sigma_{D^e_{gtT}} = \sqrt{E\left[\left(S_{gtT} - \mu_{S_{gtT}}\right)^2\right] + E\left[\left(I_{gtT} - \mu_{I_{gtT}}\right)^2\right]} = \sqrt{\mathrm{Var}(D^e_{gtT})} \quad (17)$$

Originally developed by Malcolm et al. (1959), PERT is a continuous probability distribution defined by minimum a, mode m, and maximum b values that a variable can take, where the mean of the simulated variable is given by

$$\mu = \frac{a + 4m + b}{6}. \quad (18)$$

We find PERT distribution as the appropriate simulation model for rainfall and evapotranspiration mainly because, unlike other distributions, it is bounded by their historical minimum and maximum records and would never drift to infinity, which is the case with the two variables. We bank on the flexibility of PERT, which allows for higher-order moments vis skewness and kurtosis in distribution curves, to achieve precise rainfall deficiency and actuarial premiums. Further, in a study contemporary to this one, PERT distribution were validated against time series approaches [mainly seasonal autoregressive integrated moving average (SARIMA) and its variants] where PERT distribution was found to be more appropriate in rainfall simulation (Li 2018; Shee et al. 2019). Figures 3 and 4 respectively present, for growth stages 1–4, rainfall and maize evapotranspiration PERT distributions based on raw historical data parameters (minimum, mode, and maximum) for four divisions.

5. An empirical example

Using raw historical rainfall and maize evapotranspiration data from Machakos County in Kenya and a risk modeling

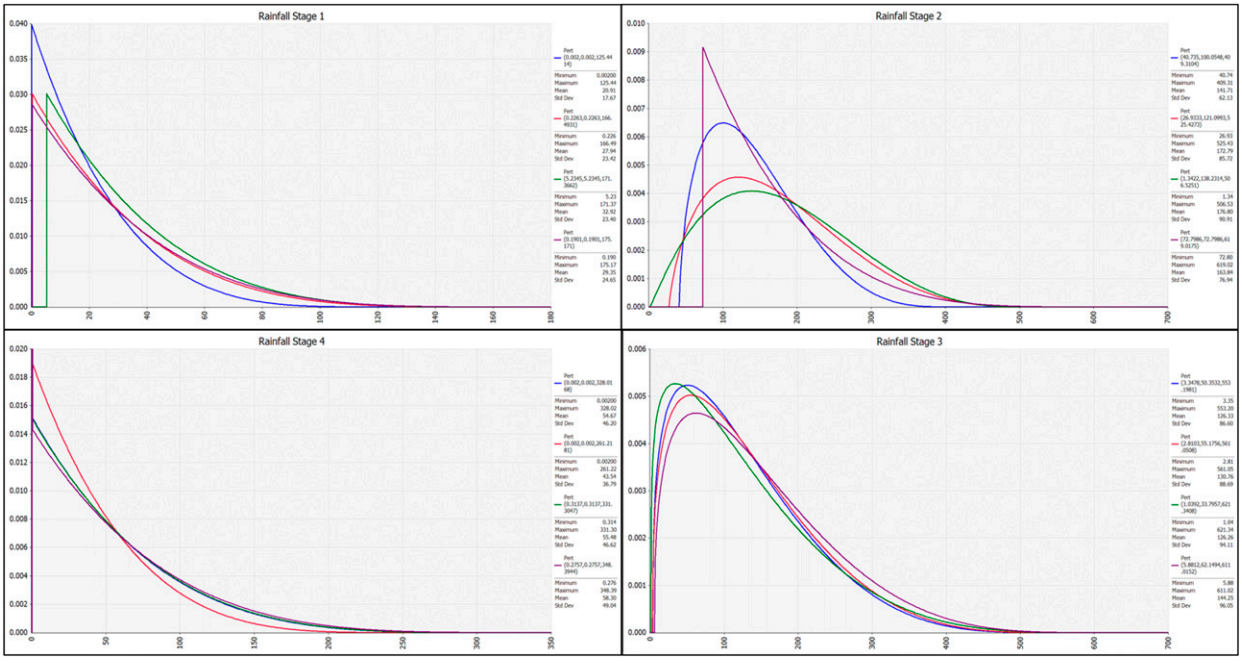

FIG. 3. For growth stages 1–4, PERT distributions for rainfall from four divisions: blue for Central Machakos, red for Yatta, green for Matungulu, and violet for Kalama. (top left) Growth stage 1 is initial stage, (top right) growth stage 2 is development stage, (bottom right) growth stage 3 is midstage, and (bottom left) growth stage 4 is late stage.

framework with @RISK software, we specify PERT Monte Carlo simulation functions for both weather variables. To capture sufficient possible values for either, as well as sufficient possible combinations of both, we run one simulation set with 10 000 iterations. Using their respective equations, we then compute stagewise random rainfall shortfalls [Eq. (7)], tick values [Eq. (8)], and indemnities [Eq. (9)]. To mitigate against intratemporal basis risks, all simulations as well as triggers,

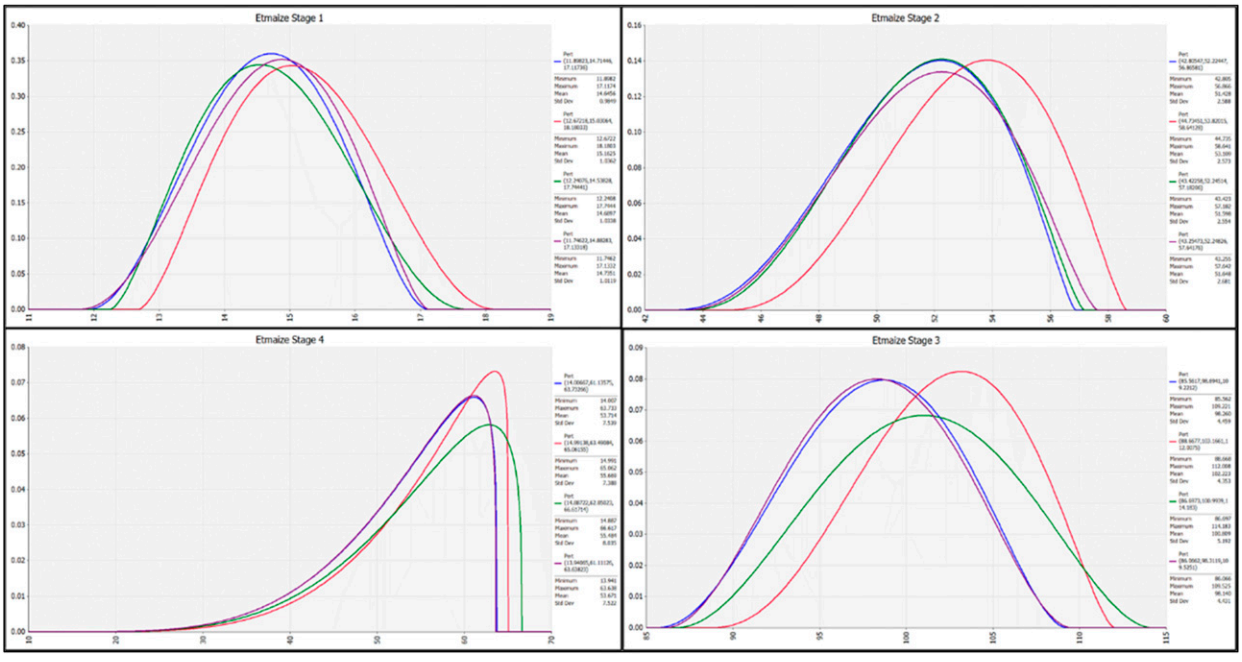

FIG. 4. As in Fig. 3, but for maize evapotranspiration (ETmaize).

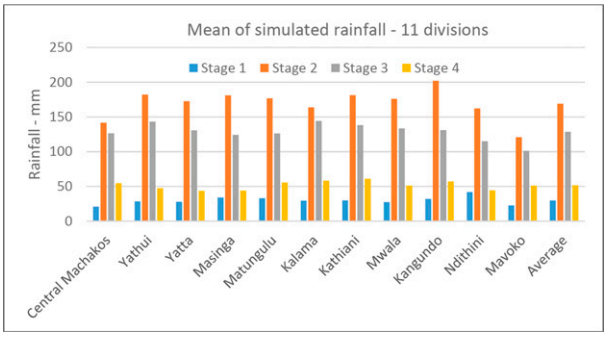

FIG. 5. Mean of simulated rainfall from the iterations.

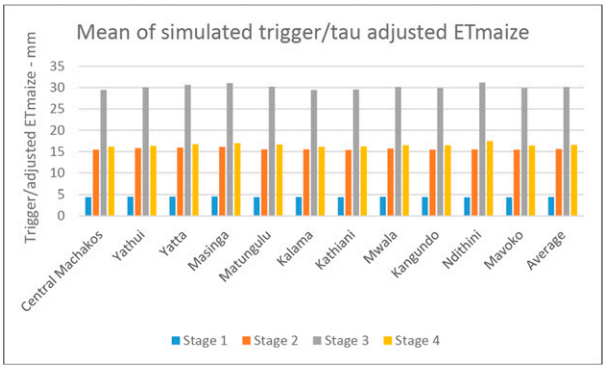

FIG. 6. Mean of adjusted maize evapotranspiration/triggers from the iterations.

rainfall shortfalls, and indemnities computations were done separately for each growth stage. We then sum up all the stagewise indemnities to get a seasonal indemnity for each iteration [Eq. (10)]. Further, we get the mean seasonal indemnity from all the iterations that gives us the actuarially fair premiums. To mitigate against spatial basis risks, we keep all of the computations and models at the division level.

a. Rainfall triggers and shortfalls

As already indicated, since both growth-stage rainfall and evapotranspiration vary over time and space, we treat them as random variables and hence simulate both. Figure 5 shows the mean of growth-stage rainfall and Fig. 6 the mean of the triggers from simulation iterations for all the 11 divisions and the average of them. The spatial correlation across the divisions can be seen in the similar and almost equal trends. In line with the raw historical data, the first stage receives the least rainfall, followed by the fourth stage. The second stage receives the highest. Figure 7 shows the distributions of simulated rainfall for Central Machakos rainfall for four growth stages with the average triggers and the percentage of entries above and below each trigger indicated. The triggers indicated here are averages from the iterations and hence should be looked at as indicative and not the ones the indemnities are based on. The fourth stage (late) had the highest payout probability where 22.2% of the cases were below the average trigger. First (initial) stage was second with 16.3% payout probability followed by third (mid-) stage, which had 10.5% payout probability. The average trigger for the second (development) stage was 15.4 mm, which was way below the minimum rainfall amount registered for that stage. This indicates that, for Central Machakos, there was no payout triggered for this stage, which is consistent with other results discussed below.

b. Tick values

As mentioned in section 4b, we define the tick value, the amount paid for each rainfall mm below the trigger, as the ratio of sum insured (principal amount for RCC) to crop evapotranspiration. In other words, the tick is the unit value of the amount of water required at each growth stage for the crop to yield optimally at the end of the season. In line with the reality where ticks vary across seasons, growth stages, and divisions, our model calculated a tick value for each growth stage and iteration that was used to compute the payout for that particular iteration, which actually represents a complete season. For illustration, Table 2 presents the mean of ticks across growth stages for all of the divisions and their average.

c. Growth stages, seasonal indemnities, and premiums

Table 3 shows average growth-stage indemnities for a loan of KES 10,000 (USD 100),[5] which was deemed sufficient for cultivation of one acre with maize and its main intercrops. The highest payouts are earned in stage 4, the late stage, with an average of KES 372. Ndithini Division had the highest (KES 451) and Kathiani had the least (KES 312). This is followed by stage 1, the initial stage, with an average of KES 158, where Central Machakos leads with KES 251 and Matungulu trails with zero payout at stage 1. Stage 3, midstage, had the third highest payouts with an average of KES 140, with Ndithini leading (KES 192) and Kalama with the least (KES 79). There were, evidently, no indemnities triggered in stage 2, the development stage, where almost all the divisions earned nil payouts apart from Masinga and Matungulu, which earned negligible amounts of KES 4 and KES 5, respectively. The results are in line with stagewise differentiation of the raw historical rainfall and maize evapotranspiration data as shown in Fig. 2. The temporospatial variations are also evidently clear in these results, with substantial payout differences across stages and divisions.

Figure 8 shows trigger and indemnity structures at growth-stage levels using Central Machakos as an example. We have 11 such structures, one for each division. The vertical delimiters indicate the average trigger points that were 4.8, 30.5, and 18.5 mm for initial, mid-, and late stages, respectively. The horizontal delimiters indicate the average payouts/indemnities as discussed in Table 3. The mechanism for the development stage shows no payouts were triggered as the rainfall for this stage was in almost all instances sufficient to meet the crop needs.

[5] The exchange rate for Kenya shillings to USD was USD 1 = KES 100, and the same applies for this paper.

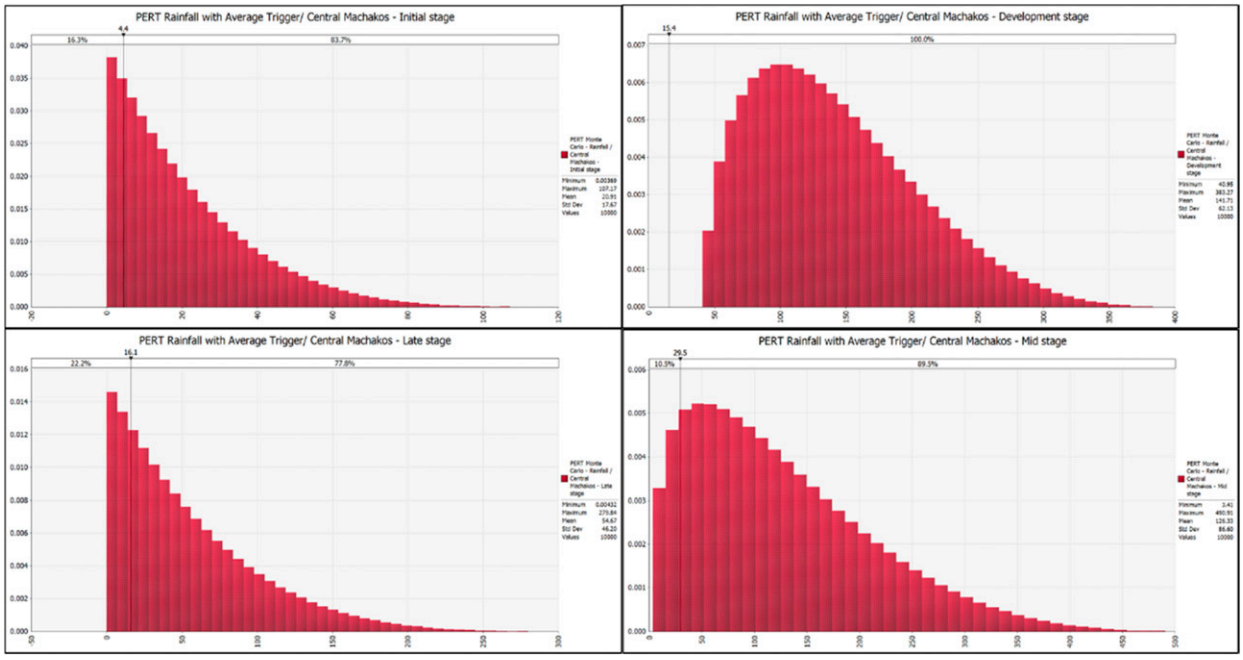

FIG. 7. Simulation output for the four growth stages of rainfall in Central Machakos showing the average trigger (30% of maize evapotranspiration) for each stage. Central Machakos is used as an example that is a depiction of simulation distribution outputs for all the other divisions.

As discussed throughout this paper, payout determination and calculation are stagewise but for ease and convenience of running the product, it is operated at seasonal level with the summation of the indemnities from all growth stages. To avoid payouts that do not make financial and economic sense to both farmers and insurance companies, we impose a minimum payout (m = KES 500) if and only if there was a payout triggered at the end of the season.

Table 4 gives a summary of the product for all 11 divisions of Machakos County. Payout probability for the product ranges from 33.14% in Matungulu to 46.83% in Mavoko, with an average of 40.25%. This is a true depiction of the rainfall and aridity variations across the divisions and the agroecological zoning of the county. In our design, we worked with a loan of KES 10,000, which represents the sum insured, which can be scaled up or down based on one's needs. With that, we calculated actuarially fair premium rates that we believe are sufficiently robust and stable. They range from 5.4% in Matungulu to 8.1% in Mavoko with an average of 6.9%. For commercial offering and markup, we set a loading factor of 25%, which is based on our previous experience with insurers and banks from the region. This increases the lowest premium to 6.8%, the highest premium to 10.1%, and the average premium to 8.6%. The rates may sound somewhat high but are justifiable given the aridity in these areas as reflected in payout probabilities that average at 40.25%.

6. Discussion

Uninsured weather risks are a major bottleneck to smallholders' productivity and access to investment credit especially when their anticipated farm produce is the main source of revenue for loan repayment. The traditional all-peril crop insurance has failed among this category of farmers mainly due to adverse selection, moral hazard, and high transactional costs from physical assessment of losses. Weather index insurance has raised the hopes of providing affordable formal insurance to smallholders by hedging their agricultural production against the main covariate risks that devastate their farms and livelihoods. While free of adverse selection and moral hazards limitations, WII products are faced with the basis risk challenge, which together with farmers' liquidity constraint has led to its low uptake.

We contribute to the literature with a new design for an improved rainfall index insurance that can be applied as standalone insurance product, or as provided in this paper, a

TABLE 2. Average tick values by growth stages and divisions (identification numbers are in parentheses).

Divisions	Stage 1	Stage 2	Stage 3	Stage 4
Central Machakos (208)	685.94	194.95	101.98	190.76
Yathui (213)	667.45	190.53	100.02	187.56
Yatta (214)	662.61	188.74	98.00	183.58
Masinga (225)	659.34	187.17	96.76	180.72
Matungulu (230)	684.12	194.29	99.46	184.94
Kalama (248)	681.92	194.15	102.10	190.91
Kathiani (251)	688.68	195.89	101.72	190.05
Mwala (252)	671.35	191.63	99.68	186.25
Kangundo (263)	683.06	195.09	100.56	187.17
Ndithini (264)	692.14	194.29	96.61	176.72
Mavoko (265)	693.45	195.02	100.37	187.68
Mean	679.10	192.88	99.75	186.03

TABLE 3. Average growth-stage indemnities for all divisions.

Division	Stage 1	Stage 2	Stage 3	Stage 4
Central Machakos	251.09	0.00	122.47	344.35
Yathui	190.94	0.00	89.34	397.93
Yatta	179.41	0.00	122.41	438.82
Masinga	162.86	4.33	189.99	411.16
Matungulu	00.00	5.11	187.00	340.55
Kalama	168.13	0.00	78.63	314.87
Kathiani	176.51	0.00	109.40	311.61
Mwala	196.66	0.00	97.21	374.88
Kangundo	166.44	0.00	165.01	337.72
Ndithini	13.01	0.00	191.75	450.86
Mavoko	229.35	0.00	186.27	373.96
Mean	157.67	0.86	139.95	372.43

bundled risk-contingent credit product. Rainfall is the most used index for WII in SSA where drought is the most important covariate risk. First, we improve the triggering mechanism by introducing the use of crop evapotranspiration (crop water requirement) as a trigger for rainfall index insurance. We believe this is a more objective way of determining the trigger, especially in SSA and other low-income countries where reliable historical farm yield data are entirely unavailable and hence impractical to predict yield using standard regression methods as is common in other parts of the world (Bucheli et al. 2020; Conradt et al. 2015; Dalhaus and Finger 2016; Dalhaus et al. 2018; Vroege et al. 2021b). Evapotranspiration has been identified in several papers as a potential weather variable in design of WII but so far there is no substantive product design particularly where crop evapotranspiration is used without yield data. Bucheli et al. (2020) compared different WII designs and conclude that evaporative stress index (ESI) was most beneficial for wheat farmers in eastern Germany. The approach would, however, not be applicable in the absence of accurate farm-level or area average yields, which is common among smallholders in SSA. von Negenborn et al. (2017) explored the influence of precipitation and evapotranspiration indices on the credit risk of farmers from Madagascar and found that weather-related part of the credit risk of farmers can be better explained by evapotranspiration than by a precipitation index. They acknowledged the potential for weather index insurance that is based on an evapotranspiration index. Blakeley et al. (2020) assessed the applicability of reference evapotranspiration and precipitation in designing WII and concluded that both are not perfect substitutes for monitoring crop deficits and that there may be space to use both for index insurance design. Beyond exploring this space, we go farther and apply Allen et al. (1998) approaches to compute specific crop evapotranspiration/water requirement from the reference evapotranspiration and use that as a trigger for rainfall index insurance. We work with maize grown by smallholders from Machakos County, Kenya, but the model can be adapted for any crop grown in any part of the globe.

Second, following Allen et al. (1998), we divide the season into four distinct crop growth stages and cumulate rainfall and evapotranspiration at these stages and hence substantially reduce intertemporal basis risk. Allen et al.'s (1998) approaches of season sequencing and evapotranspiration have been used for years in irrigation need determination

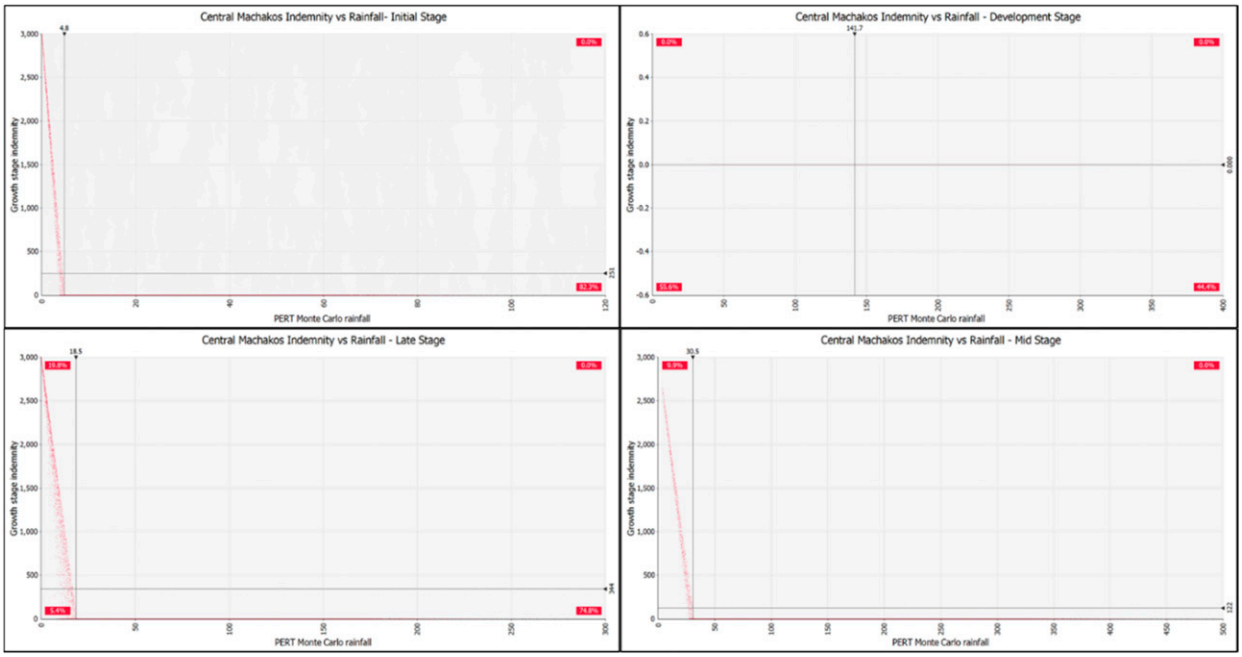

FIG. 8. Growth-stage trigger and indemnity structures, using Central Machakos as an example, for growth stages (top left) 1, (top right) 2, (bottom right) 3, and (bottom left) 4.

TABLE 4. Seasonal indemnities and insurance premiums for all divisions.

Divisions	Payout probabilities	Actuarial premiums (KES)	Actuarial premium rates	Commercial premium rates
Central Machakos	41.83%	733.3	7.3%	9.2%
Yathui	40.09%	691.6	6.9%	8.6%
Yatta	43.66%	755.1	7.6%	9.4%
Masinga	44.52%	783.8	7.8%	9.8%
Matungulu	33.14%	544.3	5.4%	6.8%
Kalama	35.43%	575.0	5.7%	7.2%
Kathiani	36.29%	611.8	6.1%	7.6%
Mwala	40.17%	683.5	6.8%	8.5%
Kangundo	40.12%	683.7	6.8%	8.5%
Ndithini	40.66%	672.0	6.7%	8.4%
Mavoko	46.83%	806.5	8.1%	10.1%
Avg	40.25%	685.5	6.9%	8.6%

and scheduling. As agronomists and biosystems engineers use the water need to determine irrigation thresholds and needs, we use it to trigger and compute indemnity. We consider the start and end of growth stages and seasons to be static over the years, with the long rain season for Machakos starting around early October until mid-January the following year. Literature on reducing intertemporal basis risk by assessing crop phenological stages is now gaining track (Blakeley et al. 2020; Dalhaus and Finger 2016; Dalhaus et al. 2018; Shi and Jiang 2016; Turvey et al. 2019). Among the proposed approaches, we feel Allen et al. (1998) would be a good candidate since it is applicable to any crop.

Third, we bundle the WII to agricultural loans and hence present an improvement of the existing RCC. There have been mixed findings on the up take of insurance bundled loans with some reporting no effect, some positive effect (Bellissa et al. 2020; Gallenstein et al. 2021; Mishra et al. 2020; Ndegwa et al. 2020), and others negative effect (Giné and Yang 2009). Inherent basis risk and complexity of WII has a negative effect on the uptake of insurance bundled credit. Our proposed design significantly improves the triggering mechanism and sequences the variables at phenotypic growth stages of the underlying crop hence reducing intertemporal basis risk. Further, the design compares crop water requirement and realized precipitation that are straightforward and easily comprehensible to the banks, insurers, and farmers.

Fourth, we adjust crop evapotranspiration with $\tau = 0.3$ to only indemnify serious drought where a crop receives below 30% of its water needs at specific stages and impose a minimum payout of KES 500 (if triggered at least once) to avoid meagre payouts that do not make economic and financial sense. To achieve greater precision in premiums calculations, we use Monte Carlo simulation with correlated PERT distribution and generate 10 000 iterations of both rainfall and crop evapotranspiration. Using @RISK software for Monte Carlo simulations, we apply spatial correlation as in Shee et al. (2019) and for the first time apply bivariate correlation between rainfall and crop evapotranspiration. This plays a major role in dealing with remaining basis risk in the WII and RCC design, especially given the spatial and bivariate correlation observed in the raw historical data. The design leads to about 40.3% average payout probability across 11 divisions with the highest being 46.8% and the lowest 33.1%. This is in harmony with the increasing aridity and recurrent drought in the county. Further, the average actuarial premium rate (before loading) across the divisions was 6.9% for a loan of KES 10,000. The highest actuarial premium rate was 8.1%, and the lowest was 5.4%.

7. Conclusions

In this paper, we present improved weather index insurance and risk-contingent credit designs ideal for the sub-Saharan Africa and other low-income economies with an abundance of small farms and absence of reliable yield data. Working with maize from Machakos County in Kenya as our case study, we develop a rainfall index insurance whose trigger is the specific crop evapotranspiration that is equal to crop water requirement. We sequence the product at crop phenotypic growth stages, which mitigates intertemporal basis risk. We also keep the product designs within divisions to control for spatial basis risk. We see some significant temporal and spatial variations in the payouts and premiums but on average, the product leads to about 40% indemnity probability and about 7% actuarial premium rate. An indemnity probability of 40% is in line with the recurrent drought and increasing aridity in the area. We also consider a premium rate of 7% acceptable given the indemnity chances and in comparison with other products offered to farmers in Africa.

Besides literature and research furtherance, our proposed product has benefits for the insurers, financial institutions, and farmers. Not only does it complement the available index insurance products but also substantially improves the triggering mechanism and hence reduces intertemporal basis risk. It hence expands and improves the options for insurers and lenders keen on expanding their portfolios among farming households, especially the rural smallholders from low-income countries where yield data is difficult to come by. This would in return enhance risk management options and credit access among smallholders, which have been proven to have investment, productivity, and welfare benefits for such households. Our proposed product leads to 40% indemnity probability and 7% actuarial premium rates. This is, by all means, a favorable product for farmers and hence, policy makers, insurers, and banks could consider our design to promote affordable insurance and insurance-linked credit to smallholder households. Further, policy makers and development practitioners who have been promoting insurance among the smallholders in the region could consider our approaches and develop products for specific crops, considering growth stages to minimize intertemporal basis risk. It also calls for development of appropriate educational materials able to cover the main concepts and yet be simple enough for the farmers in this region who mostly have low literacy and numeracy levels.

TABLE B1. Spatial correlation matrices for rainfall over divisions (208–265) and growth stages. Panel A is initial stage, panel B is development stage, panel C is midstage, and panel D is late stage.

	208	213	214	225	230	248	251	252	263	264	265
						Panel A					
208	1.000	—	—	—	—	—	—	—	—	—	—
213	0.755	1.000	—	—	—	—	—	—	—	—	—
214	0.748	0.962	1.000	—	—	—	—	—	—	—	—
225	0.677	0.767	0.831	1.000	—	—	—	—	—	—	—
230	0.839	0.840	0.890	0.802	1.000	—	—	—	—	—	—
248	0.977	0.720	0.714	0.597	0.825	1.000	—	—	—	—	—
251	0.953	0.823	0.827	0.737	0.866	0.905	1.000	—	—	—	—
252	0.834	0.878	0.881	0.689	0.878	0.809	0.922	1.000	—	—	—
263	0.858	0.833	0.838	0.672	0.866	0.814	0.943	0.970	1.000	—	—
264	0.652	0.689	0.813	0.803	0.872	0.641	0.691	0.714	0.674	1.000	—
265	0.906	0.774	0.762	0.649	0.882	0.898	0.878	0.813	0.856	0.680	1.000
						Panel D					
208	1.000	—	—	—	—	—	—	—	—	—	—
213	0.901	1.000	—	—	—	—	—	—	—	—	—
214	0.932	0.957	1.000	—	—	—	—	—	—	—	—
225	0.878	0.873	0.936	1.000	—	—	—	—	—	—	—
230	0.971	0.887	0.936	0.893	1.000	—	—	—	—	—	—
248	0.977	0.933	0.926	0.851	0.933	1.000	—	—	—	—	—
251	0.979	0.939	0.951	0.882	0.972	0.971	1.000	—	—	—	—
252	0.955	0.968	0.965	0.882	0.957	0.958	0.983	1.000	—	—	—
263	0.950	0.947	0.947	0.865	0.966	0.953	0.987	0.985	1.000	—	—
264	0.921	0.842	0.937	0.946	0.949	0.869	0.918	0.902	0.894	1.000	—
265	0.957	0.849	0.880	0.766	0.912	0.936	0.926	0.902	0.895	0.852	1.000

	208	213	214	225	230	248	251	252	263	264	265
						Panel B					
208	1.000	—	—	—	—	—	—	—	—	—	—
213	0.860	1.000	—	—	—	—	—	—	—	—	—
214	0.870	0.930	1.000	—	—	—	—	—	—	—	—
225	0.793	0.820	0.889	1.000	—	—	—	—	—	—	—
230	0.882	0.840	0.928	0.822	1.000	—	—	—	—	—	—
248	0.964	0.886	0.849	0.750	0.862	1.000	—	—	—	—	—
251	0.958	0.915	0.911	0.788	0.911	0.935	1.000	—	—	—	—
252	0.909	0.913	0.973	0.849	0.935	0.885	0.952	1.000	—	—	—
263	0.900	0.910	0.920	0.788	0.908	0.887	0.961	0.966	1.000	—	—
264	0.766	0.779	0.877	0.896	0.892	0.733	0.781	0.841	0.790	1.000	—
265	0.917	0.766	0.831	0.715	0.893	0.869	0.881	0.850	0.815	0.760	1.000
						Panel C					
208	1.000	—	—	—	—	—	—	—	—	—	—
213	0.888	1.000	—	—	—	—	—	—	—	—	—
214	0.876	0.917	1.000	—	—	—	—	—	—	—	—
225	0.736	0.739	0.880	1.000	—	—	—	—	—	—	—
230	0.897	0.825	0.911	0.764	1.000	—	—	—	—	—	—
248	0.982	0.920	0.864	0.701	0.863	1.000	—	—	—	—	—
251	0.966	0.921	0.898	0.715	0.920	0.956	1.000	—	—	—	—
252	0.932	0.923	0.965	0.801	0.936	0.915	0.957	1.000	—	—	—
263	0.921	0.928	0.897	0.692	0.913	0.915	0.971	0.963	1.000	—	—
264	0.844	0.813	0.908	0.913	0.901	0.814	0.842	0.892	0.826	1.000	—
265	0.952	0.782	0.808	0.671	0.887	0.917	0.891	0.865	0.847	0.826	1.000

TABLE B2. As in Table B1, but for maize evapotranspiration.

	208	213	214	225	230	248	251	252	263	264	265
						Panel A					
208	1.000	—	—	—	—	—	—	—	—	—	—
213	0.985	1.000	—	—	—	—	—	—	—	—	—
214	0.984	0.991	1.000	—	—	—	—	—	—	—	—
225	0.966	0.972	0.994	1.000	—	—	—	—	—	—	—
230	0.981	0.967	0.987	0.985	1.000	—	—	—	—	—	—
248	0.998	0.987	0.980	0.959	0.971	1.000	—	—	—	—	—
251	0.998	0.985	0.990	0.978	0.991	0.994	1.000	—	—	—	—
252	0.993	0.995	0.997	0.984	0.986	0.991	0.996	1.000	—	—	—
263	0.988	0.975	0.990	0.985	0.999	0.980	0.996	0.991	1.000	—	—
264	0.942	0.932	0.964	0.977	0.985	0.928	0.959	0.955	0.977	1.000	—
265	0.993	0.967	0.977	0.966	0.989	0.987	0.995	0.984	0.993	0.958	1.000
						Panel D					
208	1.000	—	—	—	—	—	—	—	—	—	—
213	0.993	1.000	—	—	—	—	—	—	—	—	—
214	0.995	0.998	1.000	—	—	—	—	—	—	—	—
225	0.991	0.995	0.998	1.000	—	—	—	—	—	—	—
230	0.996	0.992	0.996	0.992	1.000	—	—	—	—	—	—
248	0.999	0.992	0.993	0.989	0.993	1.000	—	—	—	—	—
251	0.999	0.995	0.997	0.993	0.998	0.997	1.000	—	—	—	—
252	0.996	0.999	0.999	0.995	0.996	0.994	0.998	1.000	—	—	—
263	0.996	0.993	0.996	0.992	1.000	0.994	0.999	0.997	1.000	—	—
264	0.990	0.980	0.986	0.986	0.994	0.987	0.990	0.986	0.992	1.000	—
265	0.996	0.984	0.989	0.985	0.996	0.995	0.996	0.990	0.995	0.992	1.000

	208	213	214	225	230	248	251	252	263	264	265
						Panel B					
208	1.000	—	—	—	—	—	—	—	—	—	—
213	0.975	1.000	—	—	—	—	—	—	—	—	—
214	0.965	0.993	1.000	—	—	—	—	—	—	—	—
225	0.942	0.974	0.992	1.000	—	—	—	—	—	—	—
230	0.973	0.975	0.986	0.973	1.000	—	—	—	—	—	—
248	0.996	0.970	0.954	0.926	0.955	1.000	—	—	—	—	—
251	0.995	0.982	0.981	0.961	0.991	0.983	1.000	—	—	—	—
252	0.979	0.995	0.996	0.978	0.988	0.968	0.991	1.000	—	—	—
263	0.975	0.980	0.988	0.972	0.998	0.959	0.992	0.993	1.000	—	—
264	0.915	0.928	0.949	0.954	0.959	0.898	0.935	0.936	0.944	1.000	—
265	0.990	0.956	0.952	0.930	0.977	0.980	0.989	0.964	0.975	0.924	1.000
						Panel C					
208	1.000	—	—	—	—	—	—	—	—	—	—
213	0.972	1.000	—	—	—	—	—	—	—	—	—
214	0.979	0.986	1.000	—	—	—	—	—	—	—	—
225	0.962	0.957	0.989	1.000	—	—	—	—	—	—	—
230	0.982	0.951	0.981	0.976	1.000	—	—	—	—	—	—
248	0.997	0.969	0.972	0.956	0.972	1.000	—	—	—	—	—
251	0.997	0.975	0.986	0.970	0.991	0.990	1.000	—	—	—	—
252	0.988	0.993	0.995	0.972	0.980	0.982	0.993	1.000	—	—	—
263	0.990	0.964	0.985	0.974	0.998	0.981	0.997	0.988	1.000	—	—
264	0.944	0.896	0.951	0.967	0.979	0.933	0.953	0.935	0.967	1.000	—
265	0.979	0.925	0.957	0.958	0.988	0.971	0.980	0.958	0.986	0.973	1.000

TABLE B3. Rainfall and maize evapotranspiration bivariate correlation matrices divisions (208–265) and growth stages (panels A–D).

		Rainfall										
		208	213	214	225	230	248	251	252	263	264	265
Panel A												
Maize evapotranspiration	208	−0.59	−0.53	−0.55	−0.52	−0.62	−0.56	−0.54	−0.46	−0.46	−0.58	−0.61
	213	−0.56	−0.50	−0.53	−0.48	−0.57	−0.53	−0.52	−0.42	−0.43	−0.53	−0.56
	214	−0.57	−0.54	−0.58	−0.53	−0.60	−0.53	−0.54	−0.45	−0.46	−0.59	−0.58
	225	−0.58	−0.57	−0.61	−0.56	−0.62	−0.54	−0.57	−0.49	−0.50	−0.62	−0.59
	230	−0.59	−0.57	−0.61	−0.57	−0.64	−0.55	−0.57	−0.49	−0.49	−0.62	−0.62
	248	−0.59	−0.52	−0.54	−0.50	−0.61	−0.56	−0.53	−0.44	−0.45	−0.56	−0.61
	251	−0.59	−0.55	−0.57	−0.53	−0.62	−0.55	−0.55	−0.47	−0.47	−0.59	−0.61
	252	−0.57	−0.53	−0.56	−0.52	−0.60	−0.54	−0.54	−0.45	−0.46	−0.57	−0.59
	263	−0.58	−0.57	−0.60	−0.56	−0.63	−0.55	−0.56	−0.48	−0.48	−0.61	−0.61
	264	−0.61	−0.61	−0.64	−0.60	−0.66	−0.57	−0.62	−0.53	−0.54	−0.65	−0.63
	265	−0.59	−0.55	−0.58	−0.55	−0.64	−0.56	−0.56	−0.48	−0.49	−0.61	−0.62
Panel D												
Maize evapotranspiration	208	−0.32	−0.18	−0.15	−0.17	−0.21	−0.36	−0.26	−0.21	−0.21	−0.13	−0.26
	213	−0.24	−0.11	−0.07	−0.10	−0.13	−0.28	−0.18	−0.13	−0.14	−0.06	−0.17
	214	−0.27	−0.14	−0.10	−0.13	−0.16	−0.31	−0.21	−0.16	−0.17	−0.09	−0.21
	225	−0.28	−0.15	−0.11	−0.15	−0.17	−0.32	−0.23	−0.18	−0.18	−0.10	−0.21
	230	−0.33	−0.19	−0.15	−0.18	−0.21	−0.36	−0.27	−0.22	−0.22	−0.14	−0.27
	248	−0.32	−0.18	−0.14	−0.17	−0.21	−0.35	−0.26	−0.21	−0.21	−0.13	−0.26
	251	−0.31	−0.17	−0.14	−0.17	−0.20	−0.34	−0.25	−0.20	−0.20	−0.12	−0.25
	252	−0.27	−0.14	−0.10	−0.14	−0.16	−0.31	−0.21	−0.17	−0.17	−0.09	−0.21
	263	−0.32	−0.18	−0.14	−0.17	−0.20	−0.35	−0.26	−0.21	−0.21	−0.13	−0.25
	264	−0.39	−0.25	−0.21	−0.24	−0.28	−0.42	−0.33	−0.28	−0.28	−0.19	−0.32
	265	−0.37	−0.22	−0.19	−0.21	−0.25	−0.39	−0.30	−0.25	−0.25	−0.17	−0.31

		Rainfall										
		208	213	214	225	230	248	251	252	263	264	265
Panel B												
Maize evapotranspiration	208	−0.51	−0.65	−0.62	−0.52	−0.55	−0.59	−0.54	−0.58	−0.54	−0.53	−0.46
	213	−0.51	−0.65	−0.62	−0.53	−0.56	−0.59	−0.55	−0.60	−0.55	−0.55	−0.47
	214	−0.49	−0.63	−0.61	−0.51	−0.55	−0.58	−0.53	−0.58	−0.54	−0.52	−0.45
	225	−0.49	−0.63	−0.61	−0.50	−0.55	−0.58	−0.53	−0.58	−0.54	−0.52	−0.46
	230	−0.48	−0.63	−0.59	−0.50	−0.52	−0.57	−0.51	−0.56	−0.52	−0.50	−0.43
	248	−0.52	−0.66	−0.63	−0.54	−0.57	−0.59	−0.55	−0.59	−0.55	−0.55	−0.47
	251	−0.50	−0.64	−0.60	−0.51	−0.53	−0.58	−0.53	−0.56	−0.53	−0.51	−0.44
	252	−0.48	−0.63	−0.59	−0.50	−0.53	−0.57	−0.52	−0.56	−0.52	−0.51	−0.44
	263	−0.47	−0.62	−0.58	−0.48	−0.51	−0.56	−0.51	−0.55	−0.52	−0.48	−0.42
	264	−0.54	−0.64	−0.62	−0.56	−0.58	−0.59	−0.54	−0.58	−0.54	−0.57	−0.50
	265	−0.52	−0.66	−0.62	−0.53	−0.56	−0.60	−0.55	−0.58	−0.55	−0.52	−0.47
Panel C												
Maize evapotranspiration	208	−0.44	−0.52	−0.44	−0.35	−0.40	−0.46	−0.48	−0.45	−0.48	−0.43	−0.37
	213	−0.27	−0.40	−0.31	−0.23	−0.26	−0.31	−0.33	−0.31	−0.35	−0.29	−0.20
	214	−0.35	−0.45	−0.38	−0.32	−0.33	−0.37	−0.41	−0.38	−0.41	−0.38	−0.27
	225	−0.38	−0.46	−0.42	−0.38	−0.37	−0.39	−0.44	−0.42	−0.43	−0.42	−0.31
	230	−0.47	−0.55	−0.48	−0.42	−0.43	−0.48	−0.52	−0.49	−0.50	−0.49	−0.39
	248	−0.43	−0.52	−0.44	−0.35	−0.41	−0.46	−0.48	−0.45	−0.48	−0.42	−0.36
	251	−0.42	−0.51	−0.43	−0.35	−0.39	−0.45	−0.47	−0.44	−0.47	−0.43	−0.36
	252	−0.35	−0.45	−0.37	−0.29	−0.32	−0.37	−0.40	−0.37	−0.41	−0.36	−0.28
	263	−0.44	−0.52	−0.45	−0.38	−0.40	−0.46	−0.49	−0.46	−0.48	−0.46	−0.38
	264	−0.51	−0.59	−0.55	−0.49	−0.49	−0.52	−0.57	−0.55	−0.56	−0.54	−0.44
	265	−0.53	−0.60	−0.55	−0.48	−0.50	−0.55	−0.58	−0.56	−0.57	−0.56	−0.47

One of the drawbacks of our models is the absence of historical yield data. It is therefore impossible to empirically proof basis risk reduction. Most of the modern index insurance products from the developed economies have the advantage of accessing farm-level reliable yield data and hence can assess the influence of the weather variables used on yield and therefore design more objective indices and triggers. This calls for the agricultural ministries in this region to make some effort to collect, store, and make available reliable yield data. Given the size and density of farms in the region, it will be rare that a farm-level insurance product would be developed and hence area average yield data suffice. Having said that, we also believe that satellite-based biomass estimates such as NDVI and EVI could be used as a proxy for crop yield to assess the quality of our index. This, however, is outside the scope of this paper and we leave it to future investigations. Further, an open area of future investigation is how this product would work with multiple crops or even whole farm index insurance. Further, future research could assess how the current debate on allowing for flexibility and annual variability on the start and end of growth stages and seasons would work with this approach (Conradt et al. 2015; Dalhaus et al. 2018). This should, however, not be at the expense of simplicity in design because complex WII designs face a communication hurdle and hence low acceptance and adoption in the field (Dalhaus and Finger 2016; Giné and Yang 2009; Leblois 2014; Odening et al. 2007; Odening and Shen 2014; Patt et al. 2009, 2010).

Acknowledgments. This research is part of Michael Ndegwa's doctoral dissertation at the Natural Resources Institute of University of Greenwich supported by the Vice Chancellor Scholarship. This work received financial support from the German Federal Ministry for Economic Cooperation and Development (BMZ) commissioned and administered through the Deutsche Gesellschaft für Internationale Zusammenarbeit (GIZ) Fund for International Agricultural Research (FIA), Grant 81260864. The research was also supported partly by the Global Resilience Partnership (GRP) through the Round 1 Global Resilience Challenge, supported by USAID in the context of a project titled "Satellite Technologies, Innovative and Smart Financing for Food Security (SATISFy)." The work was undertaken as part of the CGIAR Research Program on Policies, Institutions, and Markets (PIM) led by IFPRI. We also greatly appreciate Yating Ru from IFPRI for the assistance with accessing and downloading the remote sensing data used in this study. We appreciate the very helpful comments from the editor Michael Goldstein and three anonymous referees. The opinions expressed in this paper do not necessarily reflect the views of our donor or partners. Any errors that may remain are the authors' responsibility. The authors declare that they have no conflict of interest.

Data availability statement. Data analyzed in this study were a reanalysis of existing remote sensing weather data, which are openly available at the links in section 3d and locations cited in the reference section. Details of how the data were processed are also found in section 3d of this paper.

APPENDIX A

Calculating Extraterrestrial Radiation (Ra)

Extraterrestrial radiation is given by

$$\mathrm{RA_{MJ}} = \frac{24\times 60}{\pi} G_{sc} d_r \{[\omega_s \sin(\varphi)\sin(\delta)] + [\cos(\varphi)\cos(\delta)\sin(\omega_s)]\},$$

where $\mathrm{RA_{MJ}}$ is extraterrestrial radiation (MJ $\mathrm{m^{-2}\,day^{-1}}$); G_{sc} = 0.0820 MJ $\mathrm{m^{-2}\,min^{-1}}$ is solar constant; π = 3.151 59 is a mathematical constant; d_r is inverse relative Earth–sun distance given by $d_r = 1 + 0.033\cos[(2\pi/365)J]$, where J is the yearday between 1 (1 January) and 365 or 366 (31 December); φ is latitude in radians given by $(\pi/180) \times$ decimal degrees of latitude; δ_r is solar declination in radians given by $0.409\sin[(2\pi/365)J - 1.39]$; and ω_s is sunset hour angle in radians given by $\arccos[-\tan(\varphi)\tan(\delta)]$. The process above gives radiation $\mathrm{RA_{MJ}}$ in megajoules per meter squared per day, which is converted to millimeters per day by $\mathrm{RA_{mm}} = \mathrm{RA_{MJ}} \times 0.408$.

APPENDIX B

Correlation Matrices

The full spatial correlation matrices over divisions and growth stages for rainfall (Table B1) and maize evapotranspiration (Table B2) are given here. Also shown are the bivariate correlation matrices for rainfall versus evaporation over divisions for each growth stage (Table B3).

REFERENCES

Ali, W., A. Abdulai, and A. K. Mishra, 2020: Recent advances in the analysis of demand for agricultural insurance in developing and emerging countries. *Annu. Rev. Econ.*, **12**, 411–430, https://doi.org/10.1146/annurev-resource-110119-025306.

Allen, R. G., L. S. Pereira, D. Raes, and M. Smith, 1998: Meteorological data. Crop Evapotranspiration: Guidelines for computing crop requirements, FAO Irrigation and Drainage Paper 56, http://www.fao.org/3/x0490e/x0490e07.htm#chapter%203%20%20%20meteorological%20data.

Barnett, B. J., and O. Mahul, 2007: Weather index insurance for agriculture and rural areas in lower-income countries. *Amer. J. Agric. Econ.*, **89**, 1241–1247, https://doi.org/10.1111/j.1467-8276.2007.01091.x.

Beguería, S., S. M. Vicente-Serrano, F. Reig, and B. Latorre, 2014: Standardized precipitation evapotranspiration index (SPEI) revisited: Parameter fitting, evapotranspiration models, tools, datasets and drought monitoring. *Int. J. Climatol.*, **34**, 3001–3023, https://doi.org/10.1002/joc.3887.

Bellissa, R., R. Lensink, and A. Winkel, 2020: Effects of index insurance on demand and supply of credit: Evidence from Ethiopia. *Amer. J. Agric. Econ.*, **102**, 1511–1531, https://doi.org/10.1111/ajae.12105.

Benami, E., Z. Jin, M. R. Carter, A. Ghosh, R. J. Hijmans, A. Hobbs, B. Kenduiywo, and D. B. Lobell, 2021: Uniting remote sensing, crop modelling and economics for agricultural risk management. *Nat. Rev. Earth Environ.*, **2**, 140–159, https://doi.org/10.1038/s43017-020-00122-y.

Binswanger-Mkhize, H. P., 2012: Is there too much hype about index-based agricultural insurance? *J. Dev. Stud.*, **48**, 187–200, https://doi.org/10.1080/00220388.2011.625411.

Blakeley, L., S. Sweeney, G. Husak, L. Harrison, C. Funk, P. Peterson, and D. Osgood, 2020: Identifying precipitation and reference evapotranspiration trends in West Africa to support drought insurance. *Remote Sens.*, **12**, 2432, https://doi.org/10.3390/rs12152432.

Blaney, H. F., and W. D. Criddle, 1962: Determining consumptive use and irrigation water requirements. USDA Tech. Bull. 1275, 63 pp., https://naldc.nal.usda.gov/download/CAT87201264/PDF.

Bucheli, J., T. Dalhaus, and R. Finger, 2020: The optimal drought index for designing weather index insurance. *Eur. Rev. Agric. Econ.*, **48**, 573–597, https://doi.org/10.1093/erae/jbaa014.

Carter, M. R., F. Galarza, and S. Boucher, 2007: Underwriting area-based yield insurance to crowd-in credit supply and demand. *Savings Dev.*, **31**, 335–362.

——, L. Cheng, and A. Sarris, 2011: The impact of interlinked index insurance and credit contracts on financial market deepening and small farm productivity. *AAEA and NAREA Joint Annual Meeting*, Pittsburgh, PA, AAEA and NAREA, 24–26, http://www2.aueb.gr/conferences/Crete2012/papers/papers%20senior/Sarris.pdf.

——, A. de Janvry, and E. Sadoulet, 2014: Index-based weather insurance for developing countries: A review of evidence and a set of propositions for up-scaling. FERDI Working Paper 111, 42 pp., https://EconPapers.repec.org/RePEc:fdi:wpaper:1799.

Casaburi, L., and J. Willis, 2018: Time versus state in insurance: Experimental evidence from contract farming in Kenya. *Amer. Econ. Rev.*, **108**, 3778–3813, https://doi.org/10.1257/aer.20171526.

Chantarat, S., A. G. Mude, C. B. Barrett, and M. R. Carter, 2013: Designing index-based livestock insurance for managing asset risk in northern Kenya. *J. Risk Insur.*, **80**, 205–237, https://doi.org/10.1111/j.1539-6975.2012.01463.x.

——, ——, ——, and C. G. Turvey, 2017: Welfare Impacts of Index Insurance in the presence of a poverty trap. *World Dev.*, **94**, 119–138, https://doi.org/10.1016/j.worlddev.2016.12.044.

Conradt, S., R. Finger, and M. Spörri, 2015: Flexible weather index-based insurance design. *Climate Risk Manage.*, **10**, 106–117, https://doi.org/10.1016/j.crm.2015.06.003.

Critchley, W., K. Siegert, and C. Chapman, 1991: Water harvesting: A manual for the design and construction of water harvesting schemes for plant production. FAO Doc., http://www.fao.org/3/U3160E/U3160E00.htm.

Dalhaus, T., and R. Finger, 2016: Can gridded precipitation data and phenological observations reduce basis risk of weather index-based insurance? *Wea. Climate Soc.*, **8**, 409–419, https://doi.org/10.1175/WCAS-D-16-0020.1.

——, O. Musshoff, and R. Finger, 2018: Phenology information contributes to reduce temporal basis risk in agricultural weather index insurance. *Sci. Rep.*, **8**, 46, https://doi.org/10.1038/s41598-017-18656-5.

Djaman, K., and Coauthors, 2018: Crop evapotranspiration, irrigation water requirement and water productivity of maize from meteorological data under semiarid climate. *Water*, **10**, 405, https://doi.org/10.3390/w10040405.

ECMWF, 2019: ERA5 hourly data on single levels from 1979 to present. Copernicus Climate Data Store, accessed 5 July 2020, https://cds.climate.copernicus.eu/cdsapp#!/dataset/reanalysis-era5-single-levels?tab=overview.

Enenkel, M., C. Farah, C. Hain, A. White, M. Anderson, L. You, W. Wagner, and D. Osgood, 2018: What rainfall does not tell us—Enhancing financial instruments with satellite-derived soil moisture and evaporative stress. *Remote Sens.*, **10**, 1819, https://doi.org/10.3390/rs10111819.

——, and Coauthors, 2019: Exploiting the convergence of evidence in satellite data for advanced weather index insurance design. *Wea. Climate Soc.*, **11**, 65–93, https://doi.org/10.1175/WCAS-D-17-0111.1.

Funk, C., and Coauthors, 2015: The climate hazards infrared precipitation with stations—A new environmental record for monitoring extremes. *Sci. Data*, **2**, 150066, https://doi.org/10.1038/sdata.2015.66.

Gallenstein, R., J. E. Flatnes, J. Dougherty, S. Abdou, and K. Mishra, 2021: The impact of index-insured loans on credit market participation and risk-taking. *Agric. Econ.*, **52**, 141–156, https://doi.org/10.1111/agec.12611.

Giné, X., and D. Yang, 2009: Insurance, credit, and technology adoption: Field experimental evidence from Malawi. *J. Dev. Econ.*, **89** (1), 1–11, https://doi.org/10.1016/j.jdeveco.2008.09.007.

——, R. Townsend, and J. Vickery, 2008: Patterns of rainfall insurance participation in rural India. *World Bank Econ. Rev.*, **22**, 539–566, https://doi.org/10.1093/wber/lhn015.

Glauber, J. W., 2004: Crop insurance reconsidered. *Amer. J. Agric. Econ.*, **86**, 1179–1195, https://doi.org/10.1111/j.0002-9092.2004.00663.x.

Hargreaves, G. H., and A. Zohrab, 1985: Reference crop evapotranspiration from temperature. *Appl. Eng. Agric.*, **1**, 96–99, https://doi.org/10.13031/2013.26773.

——, and R. G. Allen, 2003: History and evaluation of Hargreaves evapotranspiration equation. *J. Irrig. Drain. Eng.*, **129**, 53–63, https://doi.org/10.1061/(ASCE)0733-9437(2003)129:1(53).

Hazell, P. B. R., 1992: The appropriate role of agricultural insurance in developing countries. *J. Int. Dev.*, **4**, 567–581, https://doi.org/10.1002/jid.3380040602.

Jaetzold, R., H. Schmidt, B. Hornetz, and C. Shisanya, 2010: Natural conditions and farm management information: Part C—East Kenya. *Farm Management Handbook of Kenya*, Vol. II, Brookpak Printing and Supplies, 406 pp.

Jensen, N. D., and C. B. Barrett, 2017: Agricultural index insurance for development. *Appl. Econ. Perspect. Policy*, **39**, 199–219, https://doi.org/10.1093/aepp/ppw022.

——, ——, and A. G. Mude, 2016: Index insurance quality and basis risk: Evidence from northern Kenya. *Amer. J. Agric. Econ.*, **98**, 1450–1469, https://doi.org/10.1093/ajae/aaw046.

Karlan, D., E. Kutsoati, M. McMillan, and C. Udry, 2011: Crop price indemnified loans for farmers: A pilot experiment in rural Ghana. *J. Risk Insur.*, **78**, 37–55, https://doi.org/10.1111/j.1539-6975.2010.01406.x.

——, R. Osei, I. Osei-Akoto, and C. Udry, 2014: Agricultural decisions after relaxing credit and risk constraints. *Quart. J. Econ.*, **129**, 597–652, https://doi.org/10.1093/qje/qju002.

Leblois, A., 2014: Weather index drought insurance: An ex ante evaluation for millet growers in Niger. *Environ. Resour. Econ.*, **57**, 525–551, https://doi.org/10.1007/s10640-013-9641-3.

——, and P. Quirion, 2013: Agricultural insurances based on meteorological indices: Realizations, methods and research challenges. *Meteor. Appl.*, **20**, 1–9, https://doi.org/10.1002/met.303.

Leppert, D., T. P. F. Dalhaus, and C.-J. Lagerkvist, 2021: Accounting for geographic basis risk in heat index insurance: How spatial interpolation can reduce the cost of risk. *Wea. Climate Soc.*, **13**, 273–286, https://doi.org/10.1175/WCAS-D-20-0070.1.

Li, Y., 2018: A comparison between PERT distribution and seasonal ARIMA model to forecast rainfall patterns. M.S. thesis, Dyson School of Applied Economics, Cornell University, 113 pp.,

https://ecommons.cornell.edu/bitstream/handle/1813/59471/Li_cornell_0058O_10285.pdf?sequence=1&isAllowed=y.

Liu, Y., K. Chen, and R. V. Hill, 2020: Delayed premium payment, insurance adoption, and household investment in rural China. *Amer. J. Agric. Econ.*, **102**, 1177–1197, https://doi.org/10.1002/ajae.12038.

Lorite, I. J., M. Ruiz-Ramos, C. Gabaldón-Leal, M. Cruz-Blanco, R. Porras, and C. Santos, 2018: Water management and climate change in semiarid environments. *Water Scarcity and Sustainable Agriculture in Semiarid Environment: Tools, Strategies, and Challenges for Woody Crops*, Academic Press, 3–40, https://doi.org/10.1016/B978-0-12-813164-0.00001-6.

Maeda, E. E., D. A. Wiberg, and P. K. E. Pellikka, 2011: Estimating reference evapotranspiration using remote sensing and empirical models in a region with limited ground data availability in Kenya. *Appl. Geogr.*, **31**, 251–258, https://doi.org/10.1016/j.apgeog.2010.05.011.

Malcolm, D. G., J. H. Roseboom, C. E. Clark, and W. Fazar, 1959: Application of a technique for research and development program evaluation. *Oper. Res.*, **7**, 646–669, https://doi.org/10.1287/opre.7.5.646.

Marr, A., A. Winkel, M. van Asseldonk, R. Lensink, and E. Bulte, 2016: Adoption and impact of index-insurance and credit for smallholder farmers in developing countries: A systematic review. *Agric. Finance Rev.*, **76**, 94–118, https://doi.org/10.1108/AFR-11-2015-0050.

Martin, S. W., B. J. Barnett, and K. H. Coble, 2001: Developing and pricing precipitation insurance. *J. Agric. Resour. Econ.*, **26**, 261–274.

Meyer, R., P. Hazell, and P. Varangis, 2017: Unlocking smallholder credit: Does credit-linked agricultural insurance work? International Labour Organization and the International Finance Corporation Doc., 46 pp., http://hdl.handle.net/10986/31437.

Ministry of Agriculture, Livestock and Fisheries, 2017: Climate risk profile for Machakos County. Kenya County Climate Risk Profile Series Doc., 24 pp., https://cgspace.cgiar.org/bitstream/handle/10568/96283/Machakosf_Climate_Risk_Profile_Final.pdf.

Miranda, M. J., and C. Gonzalez-Vega, 2011: Systemic risk, index insurance, and optimal management of agricultural loan portfolios in developing countries. *Amer. J. Agric. Econ.*, **93**, 399–406, https://doi.org/10.1093/ajae/aaq109.

Mishra, K., R. A. Gallenstein, M. J. Miranda, A. G. Sam, P. Toledo, and F. Mulangu, 2020: Insured loans and credit access: Evidence from a randomized field experiment in northern Ghana. *Amer. J. Agric. Econ.*, **103**, 923–943, https://doi.org/10.1111/ajae.12136.

Ndegwa, M. K., A. Shee, C. G. Turvey, and L. You, 2020: Uptake of insurance-embedded credit in presence of credit rationing: Evidence from a randomized controlled trial in Kenya. *Agric. Finance Rev.*, **80**, 745–766, https://doi.org/10.1108/AFR-10-2019-0116.

Norton, M., C. Turvey, and D. Osgood, 2012: Quantifying spatial basis risk for weather index insurance. *Risk Finance*, **14**, 20–34, https://doi.org/10.1108/15265941311288086.

Odening, M., and Z. Shen, 2014: Challenges of insuring weather risk in agriculture. *Agric. Finance Rev.*, **74**, 188–199, https://doi.org/10.1108/AFR-11-2013-0039.

——, O. Musshoff, and W. Xu, 2007: Analysis of rainfall derivatives using daily precipitation models: Opportunities and pitfalls. *Agric. Finance Rev.*, **6**, 135–156, https://doi.org/10.1108/00214660780001202.

Ozaki, V. A., 2009: Pricing farm-level agricultural insurance: A Bayesian approach. *Empir. Econ.*, **36**, 231–242, https://doi.org/10.1007/s00181-008-0193-2.

Patt, A., N. Peterson, M. Carter, M. Velez, U. Hess, and P. Suarez, 2009: Making index insurance attractive to farmers. *Mitigation Adapt. Strategies Global Change*, **14**, 737–753, https://doi.org/10.1007/s11027-009-9196-3.

——, P. Suarez, and U. Hess, 2010: How do small-holder farmers understand insurance, and how much do they want it? Evidence from Africa. *Global Environ. Change*, **20**, 153–161, https://doi.org/10.1016/j.gloenvcha.2009.10.007.

Pereira, L. S., and I. Alves, 2013: Crop water requirements. *Reference Module in Earth Systems and Environmental Sciences*, Elsevier, https://doi.org/10.1016/B978-0-12-409548-9.05129-0.

Piccinni, G., 2009: Determination of growth-stage-specific crop coefficients (K_C) of maize and sorghum. *Agric. Water Manage.*, **96**, 1698–1704, https://doi.org/10.1016/j.agwat.2009.06.024.

——, J. Ko, A. Went, D. Leskovar, T. Marek, and T. Howell, 2007: Determination of crop coefficients (K_c) for irrigation management of crops. *28th Annual Int. Irrigation Show*, San Diego, CA, Irrigation Association, 9–12.

Shee, A., and C. G. Turvey, 2012: Collateral-free lending with risk-contingent credit for agricultural development: Indemnifying loans against pulse crop price risk in India. *Agric. Econ.*, **43**, 561–574, https://doi.org/10.1111/j.1574-0862.2012.00603.x.

——, ——, and L. You, 2019: Design and rating of risk-contingent credit for balancing business and financial risks for Kenyan farmers. *Appl. Econ.*, **51**, 5447–5465, https://doi.org/10.1080/00036846.2019.1613502.

——, ——, and A. Marr, 2020: Heterogeneous demand and supply for an insurance-linked credit product in Kenya: A stated choice experiment approach. *J. Agric. Econ.*, **72**, 244–267, https://doi.org/10.1111/1477-9552.12401.

Shi, H., and Z. Jiang, 2016: The efficiency of composite weather index insurance in hedging rice yield risk: Evidence from China. *Agric. Econ.*, **47**, 319–328, https://doi.org/10.1111/agec.12232.

Shiferaw, B., B. M. Prasanna, J. Hellin, and M. Bänziger, 2011: Crops that feed the world 6. Past successes and future challenges to the role played by maize in global food security. *Food Secur.*, **3**, 307–327, https://doi.org/10.1007/s12571-011-0140-5.

Skees, J. R., and B. J. Barnett, 2006: Enhancing microfinance using index-based risk-transfer products. *Agric. Finance Rev.*, **66**, 235–250, https://doi.org/10.1108/00214660680001189.

——, P. Hazell, and M. Miranda, 1999: New approaches to public/private crop-yield insurance. World Bank Working Paper, 21 pp.

——, J. Hartell, and A. G. Murphy, 2007: Using index-based risk transfer products to facilitate micro lending in Peru and Vietnam. *Amer. J. Agric. Econ.*, **89**, 1255–1261, https://doi.org/10.1111/j.1467-8276.2007.01093.x.

Smith, V., and M. Watts, 2019: Index based agricultural insurance in developing countries: Feasibility, scalability and sustainability. *Gates Open Res.*, **3**, 65, https://doi.org/10.21955/gatesopenres.1114971.1.

Tabari, H., 2009: Evaluation of reference crop evapotranspiration equations in various climates. *Water Resour. Manage.*, **24**, 2311–2337, https://doi.org/10.1007/s11269-009-9553-8.

Tack, J., A. Barkley, and L. L. Nalley, 2015: Effect of warming temperatures on US wheat yields. *Proc. Natl. Acad. Sci. USA*, **112**, 6931–6936, https://doi.org/10.1073/pnas.1415181112.

——, ——, and N. Hendricks, 2017: Irrigation offsets wheat yield reductions from warming temperatures. *Environ. Res. Lett.*, **12**, 114027, https://doi.org/10.1088/1748-9326/aa8d27.

——, J. Lingenfelser, and S. V. K. Jagadish, 2017: Disaggregating sorghum yield reductions under warming scenarios exposes

narrow genetic diversity in US breeding programs. *Proc. Natl. Acad. Sci. USA*, **114**, 9296–9301, https://doi.org/10.1073/pnas.1706383114.

Tadesse, M. A., B. A. Shiferaw, and O. Erenstein, 2015: Weather index insurance for managing drought risk in smallholder agriculture: Lessons and policy implications for sub-Saharan Africa. *Agric. Food Econ.*, **3**, 26, https://doi.org/10.1186/s40100-015-0044-3.

Turvey, C. G., 2001: Weather derivatives for specific event risks in agriculture. *Rev. Agric. Econ.*, **23**, 333–351, https://doi.org/10.1111/1467-9353.00065.

——, V. L. Bogan, and C. Yu, 2012: Small businesses and risk contingent credit. *J. Risk Finance*, **13**, 491–506, https://doi.org/10.1108/15265941211273777.

——, A. Shee, and A. Marr, 2019: Addressing fractional dimensionality in the application of weather index insurance and climate risk financing in agricultural development: A dynamic triggering approach. *Wea. Climate Soc.*, **11**, 901–915, https://doi.org/10.1175/WCAS-D-19-0014.1.

Vicente-Serrano, S. M., S. Beguería, and J. I. López-Moreno, 2010: A multiscalar drought index sensitive to global warming: The standardized precipitation evapotranspiration index. *J. Climate*, **23**, 1696–1718, https://doi.org/10.1175/2009JCLI2909.1.

von Negenborn, F., R. Weber, and O. Musshoff, 2017: Explaining weather-related credit risk with evapotranspiration and precipitation indices. *Agric. Finance Rev.*, **78**, 246–261, https://doi.org/10.1108/AFR-07-2017-0058.

Vroege, W., A. Vrieling, and R. Finger, 2021a: Satellite support to insure farmers against extreme droughts. *Nat. Food*, **2**, 215–217, https://doi.org/10.1038/s43016-021-00244-6.

——, J. Bucheli, T. Dalhaus, M. Hirschi, and R. Finger, 2021b: Insuring crops from space: The potential of satellite-retrieved soil moisture to reduce farmers' drought risk exposure. *Eur. Rev. Agric. Econ.*, **48**, 266–314, https://doi.org/10.1093/erae/jbab010.

Wu, I.-P., 1997: A simple evapotranspiration model for Hawaii: The Hargreaves model. University of Hawai'i at Mānoa Cooperative Extension Service Engineer's Notebook No. 106, 2 pp., https://www.ctahr.hawaii.edu/oc/freepubs/pdf/EN-106.pdf.

Zhao, W., B. Liu, and Z. Zhang, 2010: Water requirements of maize in the middle Heihe River basin, China. *Agric. Water Manage.*, **97**, 215–223, https://doi.org/10.1016/j.agwat.2009.09.011.